

October 16, 2018

Nonleptonic two-body decays of single heavy baryons Λ_Q , Ξ_Q , and Ω_Q ($Q = b, c$) induced by W emission in the covariant confined quark model

Thomas Gutsche,¹ Mikhail A. Ivanov,² Jürgen G. Körner,³ and Valery E. Lyubovitskij^{1, 4, 5, 6}¹*Institut für Theoretische Physik, Universität Tübingen,**Kepler Center for Astro and Particle Physics, Auf der Morgenstelle 14, D-72076 Tübingen, Germany*²*Bogoliubov Laboratory of Theoretical Physics, Joint Institute for Nuclear Research, 141980 Dubna, Russia*³*PRISMA Cluster of Excellence, Institut für Physik,**Johannes Gutenberg-Universität, D-55099 Mainz, Germany*⁴*Departamento de Física y Centro Científico Tecnológico de Valparaíso-CCTVal,**Universidad Técnica Federico Santa María, Casilla 110-V, Valparaíso, Chile*⁵*Department of Physics, Tomsk State University, 634050 Tomsk, Russia*⁶*Laboratory of Particle Physics, Tomsk Polytechnic University, 634050 Tomsk, Russia*

We have made a survey of heavy-to-heavy and heavy-to-light nonleptonic heavy baryon two-body decays and have identified those decays that proceed solely via W -boson emission, i.e. via the tree graph contribution. Some sample decays are $\Omega_b^- \rightarrow \Omega_c^{(*)0} \rho^- (\pi^-)$, $\Omega_b^- \rightarrow \Omega^- J/\psi(\eta_c)$, $\Xi_b^{0,-} \rightarrow \Xi^{0,-} J/\psi(\eta_c)$, $\Lambda_b \rightarrow \Lambda J/\psi(\eta_c)$, $\Lambda_b \rightarrow \Lambda_c D_s^{(*)}$, $\Omega_c^0 \rightarrow \Omega^- \rho^+ (\pi^+)$ and $\Lambda_c \rightarrow p \phi$. We make use of the covariant confined quark model previously developed by us to calculate the tree graph contributions to these decays. We calculate rates, branching fractions and, for some of these decays, decay asymmetry parameters. We compare our results to experimental findings and the results of other theoretical approaches when they are available. Our main focus is on decays to final states with a lepton pair because of their clean experimental signature. For these decays we discuss two-fold polar angle decay distributions such as in the cascade decay $\Omega_b^- \rightarrow \Omega^- (\rightarrow \Xi \pi, \Lambda K^-) + J/\psi (\rightarrow \ell^+ \ell^-)$. Lepton mass effects are always included in our analysis.

PACS numbers: 12.39.Ki, 13.30.Eg, 14.20.Jn, 14.20.Mr

Keywords: relativistic quark model, light and heavy mesons and baryons, charmonium, leptons, decay rates and asymmetries

I Introduction

In the present paper we focus on the study of nonleptonic W -emission (also referred to as tree graph contributions [1]) two-body decays of single heavy baryons

$$B_1(q_1 q_2 q_3) \rightarrow B_2(q'_1 q'_2 q'_3) + M(q_m \bar{q}_{\bar{m}}) \quad (1)$$

where M stands for a pseudoscalar meson P or a vector meson V . One of the quarks in the initial baryon is heavy. A necessary condition for the contribution of the tree graph class of decays is that a light quark pair $q_i q_j = q'_i q'_j$ is shared by the parent and daughter baryon B_1 and B_2 , respectively. A sufficient condition for the tree graph class of decays is that i) q_m is not among q_1, q_2, q_3 and ii) $q_{\bar{m}}$ is not among q'_1, q'_2, q'_3 when $q_m, q_{\bar{m}}$ are not among the quarks participating in the weak interaction. For completeness we also analyze those nonleptonic modes which are contributed to by both tree graph contributions and by a specific class of W -exchange contribution which vanish in the $SU(3)$ limit.

Our investigation is limited to the decays of the lowest lying ground states. The higher lying ground-state bottom and charm baryons such as the spin 3/2 partners decay strongly or electromagnetically. For these the weak decays do occur but have tiny branching ratios and are therefore not so interesting from an experimental point of view. In this work we therefore concentrate on the weak nonleptonic decays of the lowest lying spin 1/2 ground state bottom baryons $\Lambda_b^0, \Xi_b^0, \Xi_b^-, \Omega_b^-$ and $\Lambda_c^+, \Xi_c^+, \Xi_c^0, \Omega_c^0$.

Based on the necessary and sufficient conditions formulated above we have made a search for heavy-to-heavy and heavy-to-light nonleptonic heavy baryon decays that are solely contributed to by the tree graph contributions. We have identified a number of decays in this class. Some of these decays have been seen or are expected to be seen in the near future, or upper bounds have been established for them. Although some of these tree graph decays are singly or doubly CabibboKobayashiMaskawa (CKM) suppressed the huge data sample available at the LHC on heavy baryon decays will hopefully lead to the detection of the remaining decay modes in the near future.

Nonleptonic baryon and meson decays are interesting from the point of view that they provide a testing ground for our understanding of QCD. They involve an interplay of short-distance effects from the operator product expansion

of the current-current Hamiltonian and long-distance effects from the evaluation of current-induced transition matrix elements. On the phenomenological side one can investigate the role of $1/N_c$ color loop suppression effects. The analysis of nonleptonic two-body heavy baryon decays can also contribute to the determination of CKM matrix elements if the theoretical input can be brought under control.

An analysis of the tree graph decays provides important information on the value of the heavy-to-heavy and heavy-to-light form factors $\langle B_2 | J^\mu | B_1 \rangle$ at one particular q^2 -value corresponding to the mass of the final state meson. A small final-state meson mass implies that the form factors are probed close to the maximum recoil end of the q^2 -spectrum where one has reliable predictions from light cone sum rules. The decay constants describing the mesonic part of the transition $\langle M | J^\mu | 0 \rangle$ are either experimentally available from weak or electromagnetic decays of the mesons, or are constrained from further theoretical model analysis, lattice calculations or QCD sum rule analysis.

In this paper we present a detailed analysis of the nonleptonic tree graph heavy baryon decays in the framework of our covariant confined quark model (CCQM) proposed and developed in Refs. [2]-[20]. The CCQM model is quite flexible in as much as it allows one to study mesons, baryons and even exotic states such as tetraquark states as bound states of their constituent quarks. In this approach particle transitions are calculated through Feynman diagrams involving quark loops. In the present application the current-induced baryon transitions $B_1 \rightarrow B_2$ are described by a two-loop diagram which requires a genuine two-loop calculation. The vacuum-to-meson transition involves a one-loop calculation. The high energy behavior of quark loops is tempered by nonlocal Gaussian-type vertex functions with a Gaussian-type fall-off behavior characterized by a size parameter specific to the meson and baryon in question. The nonlocal hadron-quark vertices have an interpolating current structure. In a recent refinement of our model we have incorporated quark confinement in an effective way [21]-[25]. Quark confinement is introduced at the level of Feynman diagrams and is based on an infrared regularization of the relevant quark-loop diagrams. In this way quark thresholds corresponding to free quark poles in the Green functions are removed (see details in Refs. [21]-[25]). Tree graph contributions to some of the decays treated in this paper have been discussed before in [26-28].

The paper is structured as follows. In Sec. II we provide a list of nonleptonic heavy baryon decays that proceed solely by the tree graph contribution. We classify the decays according to their CKM and color structure. In Sec. III we discuss the parameters of the effective weak Lagrangians that induce the current-induced transitions used in this paper. In Sec. IV we define the matrix elements for the nonleptonic decays $1/2^+ \rightarrow 1/2^+ 0^-(1^-)$ and $1/2^+ \rightarrow 3/2^+ 0^-(1^-)$ and relate the helicity amplitudes to the invariant amplitudes of these decay processes. In this way we obtain very compact expressions for the total rates. In Sec. V we discuss the structure of the interpolating currents that describe the interactions of light and heavy baryons with their constituent quarks. In Sec. VI we briefly describe the main features of the CCQM model and present the values of the model parameters such as the constituent quark masses that have been determined by a global fit to a multitude of decay processes. In Sec. VII we present our numerical results on the partial branching fractions of the various nonleptonic baryon decays and compare them to experimental results when they are available. We also discuss angular decay distributions for the most interesting cascade decay processes and present numerical results on the spin density matrix elements that describe the angular decay distributions. Finally, in Sec. VIII, we summarize our results.

II Classification of factorizing decays

In this section we list all nonleptonic two-body decays of the lowest lying spin-1/2 ground state heavy bottom and charm baryon decays $\Lambda_{b,c}, \Xi_{b,c}, \Omega_{b,c}$ which proceed solely via the tree graph. We exclude the higher-lying ground-state baryons which decay either strongly or electromagnetically.

The quark content of the baryon and meson states participating in the nonleptonic two-body decays is given by

$$B_1(q_1 q_2 q_3) \rightarrow B_2(q'_1 q'_2 q'_3) + M(q_m \bar{q}_{\bar{m}}). \quad (2)$$

One can formulate necessary and sufficient conditions for the decays which solely proceed via the tree graph contribution. These read

$$\begin{aligned} \text{necessary condition :} & \quad q_i q_j = q'_i q'_j \quad i, j = 1, 2, 3 \\ \text{sufficient condition :} & \quad q_m \ni q_1, q_2, q_3; \quad q_{\bar{m}} \ni q'_1, q'_2, q'_3; \\ & \quad q_m, q_{\bar{m}} \text{ not part of the effective current - current Lagrangian} \end{aligned} \quad (3)$$

We have made a survey of two-body nonleptonic bottom and charm baryon decays which are solely contributed to by the tree diagram. The results of this search are given as follows.

Bottom baryon decays:

$$\begin{aligned}
& b \rightarrow c \quad c \rightarrow s : \quad \text{color favored} \quad \Lambda_b^0 \rightarrow \Lambda_c^+ D_s^{(*)-} \\
& \quad \quad \quad \text{color suppressed} \quad \Lambda_b^0 \rightarrow \Lambda_c^0 \eta_c(J/\psi) \\
& \quad \quad \quad \Xi_b^{0,-} \rightarrow \Xi_c^{0,-} \eta_c(J/\psi) \\
& \quad \quad \quad \Omega_b^- \rightarrow \Omega_c^- \eta_c(J/\psi) \\
& b \rightarrow c \quad u \rightarrow d : \quad \text{color favored} \quad \Omega_b^- \rightarrow \Omega_c^{(*)0} \pi^-(\rho^-) \\
& \quad \quad \quad \text{color suppressed} \quad \Xi_b^- \rightarrow \Sigma^- D^{(*)0} \\
& \quad \quad \quad \Omega_b^- \rightarrow \Xi^{(*)-} D^{(*)0} \\
& X : \quad b \rightarrow c \quad c \rightarrow d \quad \text{color favored} \quad \Xi_b^0 \rightarrow \Xi_c^+ D^{(*)-} \\
& \quad \quad \quad \Omega_b^- \rightarrow \Omega_c^{(*)0} D^{(*)-} \\
& \quad \quad \quad \text{color suppressed} \quad \Lambda_b^0 \rightarrow n \eta_c(J/\psi) \\
& \quad \quad \quad \Xi_b^- \rightarrow \Sigma^- \eta_c(J/\psi) \\
& \quad \quad \quad \Xi_b^0 \rightarrow \Lambda^0(\Sigma^0) \eta_c(J/\psi) \\
& \quad \quad \quad \Omega_b^- \rightarrow \Xi^{(*)-} \eta_c(J/\psi) \\
& X : \quad b \rightarrow c \quad u \rightarrow s \quad \text{color suppressed} \quad \Xi_b^- \rightarrow \Xi^- D^{(*)0} \\
& \quad \quad \quad \Omega_b^- \rightarrow \Omega^- D^{(*)0} \\
& X : \quad b \rightarrow u \quad c \rightarrow s \quad \text{color favored} \quad \Lambda_b^0 \rightarrow p D_s^{(*)-} \\
& \quad \quad \quad \Omega_b^- \rightarrow \Xi^{*0} D_s^{(*)-} \quad (*) \\
& \quad \quad \quad \text{color suppressed} \quad \Omega_b^- \rightarrow \Omega^- \bar{D}^{(*)0} \\
& X : \quad b \rightarrow u \quad u \rightarrow d \quad \text{color suppressed} \quad \Xi_b^- \rightarrow \Sigma^- \pi^0(\eta, \eta', \rho^0, \omega) \\
& \quad \quad \quad \Omega_b^- \rightarrow \Xi^{(*)-} \pi^0(\eta, \eta', \rho^0, \omega) \\
& XX : \quad b \rightarrow u \quad c \rightarrow d \quad \text{color favored} \quad \Xi_b^0 \rightarrow \Sigma^+ D^{(*)-} \\
& \quad \quad \quad \Xi_b^- \rightarrow \Sigma^0 D^{(*)-} \quad (*) \\
& \quad \quad \quad \Omega_b^- \rightarrow \Xi^{(*)0} D^{(*)-} \\
& \quad \quad \quad \Omega_b^- \rightarrow \Xi^{(*)-} \bar{D}^{(*)0} \\
& XX : \quad b \rightarrow u \quad u \rightarrow s \quad \text{color suppressed} \quad \Xi_b^- \rightarrow \Xi^- \pi^0(\eta, \eta', \rho^0, \omega) \\
& \quad \quad \quad \Omega_b^- \rightarrow \Omega^- \pi^0(\eta, \eta', \rho^0, \omega)
\end{aligned} \tag{4}$$

Charm baryon decays:

$$\begin{aligned}
& c \rightarrow s \quad d \rightarrow u : \quad \text{color favored} \quad \Xi_c^+ \rightarrow \Xi^{*0} \pi^+(\rho^+) \quad (*) \\
& \quad \quad \quad \Omega_c^0 \rightarrow \Omega^- \pi^+(\rho^+) \\
& \quad \quad \quad \text{color suppressed} \quad \Omega_c^0 \rightarrow \Xi^{*0} \bar{K}^{(*)0} \quad (*) \\
& X : \quad c \rightarrow s \quad s \rightarrow u : \quad \text{color suppressed} \quad \Lambda_c^+ \rightarrow p \phi
\end{aligned} \tag{5}$$

We denote singly Cabibbo suppressed decays by one cross (X) and doubly Cabibbo suppressed decays by two crosses (XX). There are a number of decays which are also admitted by a W -exchange contribution which are, however, dynamically suppressed due to the Körner-Pati-Woo theorem [29, 30] in the $SU(3)$ limit. These decays are marked by an asterix (*). We also do not list W -emission contributions where the flavor symmetries of the initial and final spectator quarks do not match, i.e. where one has $[q_i q_j] \rightarrow \{q'_i q'_j\}$ such as in $\Lambda_b^0 \rightarrow \Sigma^0 J/\psi$ or in $\Xi_b^0 \rightarrow \Xi_c^{\prime(*)+} D^{(*)-}$.

III Effective Nonleptonic Weak Lagrangians

In this section we list the effective nonleptonic weak Lagrangians, which will be used for the calculation of heavy baryon decays in present paper. Here and in the following $V_{q_1 q_2}$ are Cabibbo-Kabayashi-Maskawa (CKM) matrix elements. In our manuscript we use the following set of CKM matrix elements:

$$\begin{aligned}
V_{ud} &= 0.97425, \quad V_{us} = 0.2252, \quad V_{ub} = 0.00389, \\
V_{cd} &= 0.230, \quad V_{cs} = 0.974642, \quad V_{cb} = 0.0406.
\end{aligned} \tag{6}$$

We are dealing with the quark level transitions (i) $b \rightarrow \bar{c}u$, $b \rightarrow \bar{c}s$, $c \rightarrow \bar{s}u$ (CKM favored), (ii) $b \rightarrow \bar{c}d$, $b \rightarrow \bar{u}s$, $b \rightarrow \bar{c}s$, $b \rightarrow \bar{u}d$, $c \rightarrow \bar{s}u$ (CKM singly suppressed), and (iii) $b \rightarrow \bar{u}s$, $b \rightarrow \bar{u}d$ (CKM doubly suppressed).

1. $b \rightarrow \bar{c}u$ and $b \rightarrow \bar{u}s$ transition with $q = d, s$ (CKM favored: $b \rightarrow \bar{c}u$, CKM suppressed: $b \rightarrow \bar{c}s$, $b \rightarrow \bar{u}s$,

CKM doubly suppressed: $b \rightarrow u\bar{c}d$):

$$\mathcal{L}_{\text{eff}} = \frac{G_F}{\sqrt{2}} \left[V_{cb}^\dagger V_{uq} (C_1 Q_1 + C_2 Q_2) + V_{ub}^\dagger V_{cq} (C_1 \tilde{Q}_1 + C_2 \tilde{Q}_2) \right] + \text{H.c.} \quad (7)$$

where Q_i and \tilde{Q}_i is the set of flavor-changing effective four-quark $b \rightarrow c\bar{u}d(s)$ and $b \rightarrow u\bar{c}d(s)$ operators

$$\begin{aligned} Q_1 &= (\bar{c}^{a_1} O^\mu b^{a_2}) (\bar{q}^{a_2} O_\mu u^{a_1}), & Q_2 &= (\bar{c}^{a_1} O^\mu b^{a_1}) (\bar{q}^{a_2} O_\mu u^{a_2}), \\ \tilde{Q}_1 &= (\bar{u}^{a_1} O^\mu b^{a_2}) (\bar{q}^{a_2} O_\mu c^{a_1}), & \tilde{Q}_2 &= (\bar{u}^{a_1} O^\mu b^{a_1}) (\bar{q}^{a_2} O_\mu c^{a_2}), \end{aligned} \quad (8)$$

$O^\mu = \gamma^\mu(1 - \gamma^5)$, C_i is the set of Wilson coefficients [31–33]:

$$C_1 = -0.25, \quad C_2 = 1.1. \quad (9)$$

The quark-level matrix elements contributing to the bottom-charm baryon and bottom-up baryon transitions are given by

$$M(b \rightarrow c\bar{u}q) = \frac{G_F}{\sqrt{2}} C_{\text{eff}}^{(bc)} V_{cb}^\dagger V_{uq} (\bar{c} O^\mu b) (\bar{q} O_\mu u), \quad M(b \rightarrow q\bar{u}c) = \frac{G_F}{\sqrt{2}} C_{\text{eff}}^{(bq)} V_{cb}^\dagger V_{uq} (\bar{q} O^\mu b) (\bar{c} O_\mu u) \quad (10)$$

and

$$M(b \rightarrow u\bar{c}q) = \frac{G_F}{\sqrt{2}} \tilde{C}_{\text{eff}}^{(bu)} V_{ub}^\dagger V_{cq} (\bar{u} O^\mu b) (\bar{q} O_\mu c), \quad M(b \rightarrow c\bar{u}q) = \frac{G_F}{\sqrt{2}} \tilde{C}_{\text{eff}}^{(bc)} V_{ub}^\dagger V_{cq} (\bar{u} O^\mu b) (\bar{q} O_\mu c), \quad (11)$$

where

$$C_{\text{eff}}^{(bc)} = \tilde{C}_{\text{eff}}^{(bu)} = \xi C_1 + C_2, \quad C_{\text{eff}}^{(bq)} = \tilde{C}_{\text{eff}}^{(bc)} = C_1 + \xi C_2. \quad (12)$$

2. $b \rightarrow c\bar{c}q$ transition with $q = d, s$ (CKM favored: $b \rightarrow c\bar{c}s$, CKM suppressed: $b \rightarrow c\bar{c}d$):

$$\mathcal{L}_{\text{eff}} = V_{cb} V_{cq}^\dagger \sum_{i=1}^6 C_i Q_i + \text{H.c.}, \quad (13)$$

where the Q_i are the set of effective four-quark flavor-changing $b \rightarrow q$ operators

$$\begin{aligned} Q_1 &= (\bar{c}^{a_1} O^\mu b^{a_2}) (\bar{q}^{a_2} O_\mu c^{a_1}), & Q_4 &= (\bar{q}^{a_1} O^\mu b^{a_2}) (\bar{c}^{a_2} O_\mu c^{a_1}), \\ Q_2 &= (\bar{c}^{a_1} O^\mu b^{a_1}) (\bar{q}^{a_2} O_\mu c^{a_2}), & Q_5 &= (\bar{s}^{a_1} O^\mu b^{a_1}) (\bar{c}^{a_2} \tilde{O}_\mu c^{a_2}), \\ Q_3 &= (\bar{q}^{a_1} O^\mu b^{a_1}) (\bar{c}^{a_2} O_\mu c^{a_2}), & Q_6 &= (\bar{q}^{a_1} O^\mu b^{a_2}) (\bar{c}^{a_2} \tilde{O}_\mu c^{a_1}), \end{aligned} \quad (14)$$

with $\tilde{O}^\mu = \gamma^\mu(1 + \gamma^5)$. The respective Wilson coefficients are [32]:

$$C_1 = -0.257, \quad C_2 = 1.009, \quad C_3 = -0.005, \quad C_4 = -0.078, \quad C_5 \simeq 0, \quad C_6 = 0.001. \quad (15)$$

The quark-level matrix elements contributing to the bottom-charm baryon and bottom-down(strange) baryon transitions are given by

$$M(b \rightarrow c\bar{c}q) = \frac{G_F}{\sqrt{2}} C_{\text{eff}}^{(bc)} V_{cb} V_{cq}^\dagger (\bar{c} O^\mu b) (\bar{q} O_\mu c), \quad (16)$$

$$M(b \rightarrow q\bar{c}c) = \frac{G_F}{\sqrt{2}} C_{\text{eff}}^{(bq)} V_{cb} V_{cq}^\dagger (\bar{q} O^\mu b) (\bar{c} O_\mu c), \quad (17)$$

where

$$C_{\text{eff}}^{(bc)} = \xi(C_1 + C_3 + C_5) + (C_2 + C_4 + C_6). \quad (18)$$

and

$$C_{\text{eff}}^{(bq)} = C_1 + C_3 + C_5 + \xi(C_2 + C_4 + C_6). \quad (19)$$

3. $c \rightarrow s\bar{q}u$ transition with $q = d, s$ (CKM favored: $c \rightarrow s\bar{d}u$, CKM suppressed: $c \rightarrow s\bar{s}u$):

$$\mathcal{L}_{\text{eff}} = \frac{G_F}{\sqrt{2}} V_{cs}^\dagger V_{uq} (C_1 Q_1 + C_2 Q_2) + \text{H.c.} \quad (20)$$

Q_i is the set of flavor-changing effective four-quark $c \rightarrow s$ operators

$$Q_1 = (\bar{s}^{a_1} O^\mu c^{a_1}) (\bar{u}^{a_2} O_\mu q^{a_2}), \quad Q_2 = (\bar{s}^{a_1} O^\mu c^{a_2}) (\bar{u}^{a_2} O_\mu q^{a_1}), \quad (21)$$

where

$$C_1 = 1.26, \quad C_2 = -0.51. \quad (22)$$

The quark-level matrix elements contributing to the charm-to-nonstrange (e.g., $\Lambda_c \rightarrow p\phi$) and charm-to-strange baryon decay (e.g., $\Lambda_c \rightarrow \Lambda\pi^+$) are given by

$$M(c \rightarrow u\bar{s}s) = \frac{G_F}{\sqrt{2}} C_{\text{eff}}^{(cu)} V_{cs}^\dagger V_{us} (\bar{u} O_\mu c) (\bar{s} O^\mu s), \quad (23)$$

where

$$C_{\text{eff}}^{(cu)} = C_2 + \xi C_1 \quad (24)$$

and

$$M(c \rightarrow s\bar{d}u) = \frac{G_F}{\sqrt{2}} C_{\text{eff}}^{(cs)} V_{cs}^\dagger V_{ud} (\bar{s} O_\mu c) (\bar{u} O^\mu d), \quad (25)$$

with

$$C_{\text{eff}}^{(cs)} = C_1 + \xi C_2. \quad (26)$$

4. $b \rightarrow u\bar{u}q$ transition (CKM singly suppressed: $b \rightarrow u\bar{u}d$, doubly suppressed: $b \rightarrow u\bar{u}s$):

$$\mathcal{L}_{\text{eff}} = \frac{G_F}{\sqrt{2}} V_{ub}^\dagger V_{uq} (C_1 Q_1 + C_2 Q_2) + \text{H.c.} \quad (27)$$

Q_i is the set of flavor-changing effective four-quark $b \rightarrow u$ operators

$$Q_1 = (\bar{u}^{a_1} O^\mu b^{a_1}) (\bar{q}^{a_2} O_\mu u^{a_2}), \quad Q_2 = (\bar{u}^{a_1} O^\mu b^{a_2}) (\bar{q}^{a_2} O_\mu u^{a_1}), \quad (28)$$

here

$$C_1 = 1.26, \quad C_2 = -0.51. \quad (29)$$

The quark-level matrix elements contributing to the $\Xi_b^- \rightarrow \Sigma^- \pi^0(\eta, \eta', \rho^0, \omega)$ and $\Xi_b^- \rightarrow \Xi^- \pi^0(\eta, \eta', \rho^0, \omega)$ are given by

$$M(b \rightarrow q\bar{u}u) = \frac{G_F}{\sqrt{2}} C_{\text{eff}}^{(bq)} V_{ub}^\dagger V_{uq} (\bar{q} O_\mu b) (\bar{u} O^\mu u), \quad (30)$$

where

$$C_{\text{eff}}^{(bq)} = C_2 + \xi C_1. \quad (31)$$

The color factor $\xi = 1/N_c$ will be set to zero in all matrix elements, i.e. we keep only the leading term in the $1/N_c$ -expansion.

IV Matrix elements, helicity amplitudes and rate expressions

The matrix element of the exclusive decay $B_1(p_1, \lambda_1) \rightarrow B_2(p_2, \lambda_2) + M(q, \lambda_M)$ is defined by

$$M(B_1 \rightarrow B_2 + M) = \frac{G_F}{\sqrt{2}} V_{ij} V_{kl}^\dagger C_{\text{eff}} f_M M_M \langle B_2 | \bar{q}_2 O_\mu q_1 | B_1 \rangle \epsilon^{\dagger \mu}(\lambda_M), \quad (32)$$

where $M = V, P$ stands for the vector and pseudoscalar mesons. M_M and f_M are the respective masses M_V, M_P and leptonic decay constants f_V, f_P . The Dirac string O^μ is defined by $O^\mu = \gamma^\mu(1 - \gamma^5)$.

The hadronic matrix element $\langle B_2 | \bar{q}_2 O^\mu q_1 | B_1 \rangle$ is expressed in terms of six ($1/2^+ \rightarrow 1/2^+$) or eight ($1/2^+ \rightarrow 3/2^+$), dimensionless invariant form factors $F_i^{V/A}(q^2)$, viz.

- Transition $\frac{1}{2}^+ \rightarrow \frac{1}{2}^+$:

$$\begin{aligned} \langle B_2 | \bar{q}_2 \gamma_\mu q_1 | B_1 \rangle &= \bar{u}(p_2, s_2) \left[\gamma_\mu F_1^V(q^2) - i\sigma_{\mu\nu} \frac{q_\nu}{M_1} F_2^V(q^2) + \frac{q_\mu}{M_1} F_3^V(q^2) \right] u(p_1, s_1) \\ \langle B_2 | \bar{q}_2 \gamma_\mu \gamma_5 q_1 | B_1 \rangle &= \bar{u}(p_2, s_2) \left[\gamma_\mu F_1^A(q^2) - i\sigma_{\mu\nu} \frac{q_\nu}{M_1} F_2^A(q^2) + \frac{q_\mu}{M_1} F_3^A(q^2) \right] \gamma_5 u(p_1, s_1) \end{aligned}$$

- Transition $\frac{1}{2}^+ \rightarrow \frac{3}{2}^+$:

$$\begin{aligned} \langle B_2^* | \bar{q}_2 \gamma_\mu q_1 | B_1 \rangle &= \bar{u}^\alpha(p_2, s_2) \left[g_{\alpha\mu} F_1^V(q^2) + \gamma_\mu \frac{p_{1\alpha}}{M_1} F_2^V(q^2) + \frac{p_{1\alpha} p_{2\mu}}{M_1^2} F_3^V(q^2) + \frac{p_{1\alpha} q_\mu}{M_1^2} F_4^V(q^2) \right] \gamma_5 u(p_1, s_1) \\ \langle B_2^* | \bar{q}_2 \gamma_\mu \gamma_5 q_1 | B_1 \rangle &= \bar{u}^\alpha(p_2, s_2) \left[g_{\alpha\mu} F_1^A(q^2) + \gamma_\mu \frac{p_{1\alpha}}{M_1} F_2^A(q^2) + \frac{p_{1\alpha} p_{2\mu}}{M_1^2} F_3^A(q^2) + \frac{p_{1\alpha} q_\mu}{M_1^2} F_4^A(q^2) \right] u(p_1, s_1) \end{aligned}$$

where $\sigma_{\mu\nu} = (i/2)(\gamma_\mu \gamma_\nu - \gamma_\nu \gamma_\mu)$ and all γ matrices are defined as in Bjorken-Drell. We use the same notation for the form factors $F_i^{V/A}$ in all transitions even though their numerical values are different.

Next we express the vector and axial helicity amplitudes $H_{\lambda_2 \lambda_M}$ in terms of the invariant form factors $F_i^{V/A}$, where $\lambda_M = t, \pm 1, 0$ and $\lambda_2 = \pm 1/2, \pm 3/2$ are the helicity components of the meson M ($M = P, V$) and the baryon B_2 , respectively. We need to calculate the expressions

$$H_{\lambda_2 \lambda_M} = \langle B_2(p_2, \lambda_2) | \bar{q}_2 O_\mu q_1 | B_1(p_1, \lambda_1) \rangle \epsilon^{\dagger \mu}(\lambda_M) = H_{\lambda_2 \lambda_M}^V - H_{\lambda_2 \lambda_M}^A \quad (33)$$

where we split the helicity amplitudes into their vector and axial parts. For the color enhanced decays the operator $\bar{q}_2 O_\mu q_1$ represents a charged current transition while the operator $\bar{q}_2 O_\mu q_1$ describes a neutral current transition for the color suppressed decays. We shall work in the rest frame of the baryon B_1 with the baryon B_2 moving in the positive z -direction: $p_1 = (M_1, \vec{0})$, $p_2 = (E_2, 0, 0, |\mathbf{p}_2|)$ and $q = (q_0, 0, 0, -|\mathbf{p}_2|)$. The helicities of the three particles are related by $\lambda_1 = \lambda_2 - \lambda_M$. We use the notation $\lambda_P = \lambda_t = 0$ for the scalar ($J = 0$) contribution to set the helicity label apart from $\lambda_V = 0$ used for the longitudinal component of the $J = 1$ vector meson. One has

- Transition $\frac{1}{2}^+ \rightarrow \frac{1}{2}^+$: $H_{-\lambda_2, -\lambda_M}^V = +H_{\lambda_2, \lambda_M}^V$ and $H_{-\lambda_2, -\lambda_M}^A = -H_{\lambda_2, \lambda_M}^A$.

$$\begin{aligned} H_{\frac{1}{2}t}^V &= \sqrt{Q_+/q^2} \left(F_1^V M_- + F_3^V \frac{q^2}{M_1} \right) & H_{\frac{1}{2}t}^A &= \sqrt{Q_-/q^2} \left(F_1^A M_+ - F_3^A \frac{q^2}{M_1} \right) \\ H_{\frac{1}{2}0}^V &= \sqrt{Q_-/q^2} \left(F_1^V M_+ + F_2^V \frac{q^2}{M_1} \right) & H_{\frac{1}{2}0}^A &= \sqrt{Q_+/q^2} \left(F_1^A M_- - F_2^A \frac{q^2}{M_1} \right) \\ H_{\frac{1}{2}1}^V &= \sqrt{2Q_-} \left(-F_1^V - F_2^V \frac{M_+}{M_1} \right) & H_{\frac{1}{2}1}^A &= \sqrt{2Q_+} \left(-F_1^A + F_2^A \frac{M_-}{M_1} \right) \end{aligned}$$

- Transition $\frac{1}{2}^+ \rightarrow \frac{3}{2}^+$: $H_{-\lambda_2, -\lambda_M}^V = -H_{\lambda_2, \lambda_M}^V$ and $H_{-\lambda_2, -\lambda_M}^A = +H_{\lambda_2, \lambda_M}^A$.

$$\begin{aligned}
H_{\frac{1}{2}t}^V &= -\sqrt{\frac{2}{3} \cdot \frac{Q_+}{q^2}} \frac{Q_-}{2M_1M_2} \left(F_1^V M_1 - F_2^V M_+ + F_3^V \frac{M_+M_- - q^2}{2M_1} + F_4^V \frac{q^2}{M_1} \right) \\
H_{\frac{1}{2}0}^V &= -\sqrt{\frac{2}{3} \cdot \frac{Q_-}{q^2}} \left(F_1^V \frac{M_+M_- - q^2}{2M_2} - F_2^V \frac{Q_+M_-}{2M_1M_2} + F_3^V \frac{|\mathbf{p}_2|^2}{M_2} \right) \\
H_{\frac{1}{2}1}^V &= \sqrt{\frac{Q_-}{3}} \left(F_1^V - F_2^V \frac{Q_+}{M_1M_2} \right) \quad H_{\frac{3}{2}1}^V = -\sqrt{Q_-} F_1^V \\
H_{\frac{1}{2}t}^A &= \sqrt{\frac{2}{3} \cdot \frac{Q_-}{q^2}} \frac{Q_+}{2M_1M_2} \left(F_1^A M_1 + F_2^A M_- + F_3^A \frac{M_+M_- - q^2}{2M_1} + F_4^A \frac{q^2}{M_1} \right) \\
H_{\frac{1}{2}0}^A &= \sqrt{\frac{2}{3} \cdot \frac{Q_+}{q^2}} \left(F_1^A \frac{M_+M_- - q^2}{2M_2} + F_2^A \frac{Q_-M_+}{2M_1M_2} + F_3^A \frac{|\mathbf{p}_2|^2}{M_2} \right) \\
H_{\frac{1}{2}1}^A &= \sqrt{\frac{Q_+}{3}} \left(F_1^A - F_2^A \frac{Q_-}{M_1M_2} \right) \quad H_{\frac{3}{2}1}^A = \sqrt{Q_+} F_1^A
\end{aligned}$$

We use the abbreviations $M_{\pm} = M_1 \pm M_2$, $Q_{\pm} = M_{\pm}^2 - q^2$, $|\mathbf{p}_2| = \lambda^{1/2}(M_1^2, M_2^2, q^2)/(2M_1)$.

For the decay width one finds

$$\Gamma(B_1 \rightarrow B_2 + M) = \frac{G_F^2}{32\pi} \frac{|\mathbf{p}_2|}{M_1^2} |V_{ij}V_{kl}^\dagger|^2 C_{\text{eff}}^2 f_M^2 M_M^2 \mathcal{H}_N \quad (34)$$

where we denote the sum of the squared moduli of the helicity amplitudes by

$$\mathcal{H}_N = \sum_{\lambda_2, \lambda_M} |H_{\lambda_2, \lambda_M}|^2. \quad (35)$$

We have chosen to label the sum of the squared moduli of the helicity amplitudes by the subscript N since \mathcal{H}_N is the common divisor needed for the normalization of the spin density matrix elements to be discussed in Sec. VII. The sum over the helicities of the daughter baryon runs over $\lambda_2 = \pm 1/2$ and $\lambda_2 = \pm 1/2, \pm 3/2$ for the $(1/2^+ \rightarrow 1/2^+)$ and $(1/2^+ \rightarrow 3/2^+)$ transitions, respectively. For the vector meson case $M = V$ one sums over $\lambda_V = 0, \pm 1$ and for the pseudoscalar meson case $M = P$ one has the single value $\lambda_P = 0$. Angular momentum conservation dictates the constraint $|\lambda_2 - \lambda_M| \leq 1/2$.

V Interpolating three-quark currents of baryons and quantum numbers

We use the following generic notation for the baryonic interpolating currents:

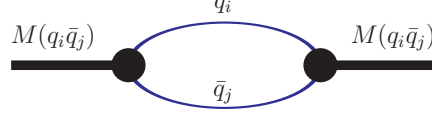
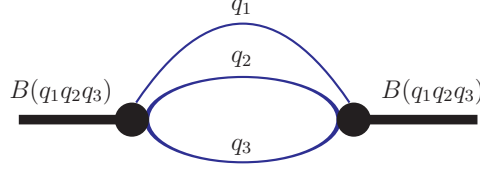
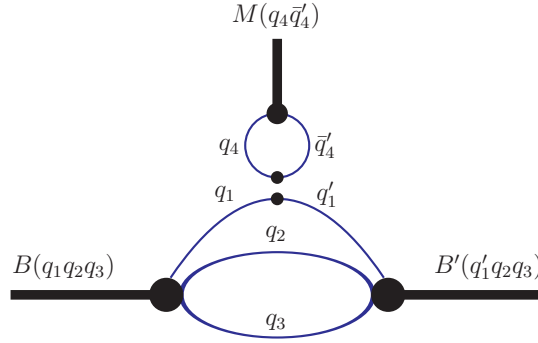
1. Spin-parity $J^P = \frac{1}{2}^+$:

$$J = \varepsilon^{a_1 a_2 a_3} J^{a_1 a_2 a_3}, \quad J^{a_1 a_2 a_3} = \Gamma_1 q_{m_1}^{a_1} q_{m_2}^{a_2} C \Gamma_2 q_{m_3}^{a_3}, \quad (36)$$

2. Spin-parity $J^P = \frac{3}{2}^+$:

$$J_\mu = \varepsilon^{a_1 a_2 a_3} J_\mu^{a_1 a_2 a_3}, \quad J_\mu^{a_1 a_2 a_3} = q_{m_1}^{a_1} q_{m_2}^{a_2} C \gamma_\mu q_{m_3}^{a_3} \quad (37)$$

where Γ_1 and Γ_2 are Dirac strings; a_i and m_i are color and flavor indices, respectively. The interpolating currents and quantum numbers of the baryons needed in this paper are summarized in Table I. As indicated in the first entry of Table I we use a superposition of two possible currents (vector and tensor) for the proton as motivated by nucleon phenomenology.

FIG. 1: Diagram representing the mass operator of a $M(q_i \bar{q}_j)$ meson.FIG. 2: Diagram representing the mass operator of a $B(q_1 q_2 q_3)$ baryon.FIG. 3: Factorizing diagram describing the $B(q_1 q_2 q_3) \rightarrow B'(q'_1 q_2 q_3) + M(q_4 \bar{q}'_4)$ transition.

The Lagrangian describing the coupling of a baryon with its constituent quarks is constructed using a nonlocal extension of the interpolating currents in Eqs. (36) and (37) (see details in Refs. [2]-[13],[25, 34]). In particular, the interaction Lagrangian for the $\frac{1}{2}^+$ baryon $B(q_1 q_2 q_3)$ composed of constituent quarks q_1, q_2 , and q_3 is written as

$$B(q_1 q_2 q_3) : \quad \mathcal{L}_{\text{int}}^B(x) = g_B \bar{B}(x) \cdot J_B(x) + \text{H.c.},$$

$$J_B(x) = \int dx_1 \int dx_2 \int dx_3 F_B(x; x_1, x_2, x_3) \varepsilon^{a_1 a_2 a_3} \Gamma_1 q_{m_1}^{a_1}(x_1) q_{m_2}^{a_2}(x_2) C \Gamma_2 q_{m_3}^{a_3}(x_3), \quad (38)$$

We treat each of the three constituent quarks as separate dynamic entities, i.e. we do not use the quark-diquark approximation for baryons as done in many applications. The propagators $S_q(k) = 1/(m_q - \not{k})$ for quarks of all flavors $q = u, d, s, c, b$ are taken in the form of free fermion propagators. The constituent quark masses m_q were fixed in a previous analysis of a multitude of hadronic processes (see, e.g., Refs. [8, 11]). By analogy we treat mesons as bound states of constituent quarks, i.e. we construct respective nonlocal Lagrangians for the mesons interacting with their constituent quarks (see details in Refs. [21]-[23]). The compositeness condition of Salam and Weinberg [14] gives a constraint equation between the coupling factors g_B and the size parameters Λ_B characterizing the nonlocal distribution $F_B(x; x_1, x_2, x_3)$. The constraint equation follows from the calculation of the mass operators for mesons (Fig. 1) and baryons (Fig. 2). As size parameters we use the values listed in Sec. VI for the nucleon, light hyperons, single charm and single heavy baryons, respectively.

TABLE I: Interpolating currents and quantum numbers of baryons

Baryon	J^P	J^{abc}	Mass (MeV)
p	$\frac{1}{2}^+$	$(1 - x_N)\gamma^\mu\gamma^5 d^a u^b C\gamma_\mu u^c$ $+ x_N\sigma^{\mu\nu}\gamma^5 d^a u^b C\sigma_{\mu\nu} u^c, \quad x_N = 0.8$	938.27
n	$\frac{1}{2}^+$	$(1 - x_N)\gamma^\mu\gamma^5 u^a d^b C\gamma_\mu d^c$ $+ x_N\sigma^{\mu\nu}\gamma^5 u^a d^b C\sigma_{\mu\nu} d^c, \quad x_N = 0.8$	939.57
Λ	$\frac{1}{2}^+$	$s^a u^b C\gamma_5 d^c$	1115.68
Σ^+	$\frac{1}{2}^+$	$\gamma^\mu\gamma^5 s^a u^b C\gamma_\mu u^c$	1189.37
Σ^0	$\frac{1}{2}^+$	$\sqrt{2}\gamma^\mu\gamma^5 s^a u^b C\gamma_\mu d^c$	1192.64
Σ^-	$\frac{1}{2}^+$	$\gamma^\mu\gamma^5 s^a d^b C\gamma_\mu d^c$	1197.45
Ξ^0	$\frac{1}{2}^+$	$\gamma^\mu\gamma^5 u^a s^b C\gamma_\mu s^c$	1314.86
Ξ^-	$\frac{1}{2}^+$	$\gamma^\mu\gamma^5 d^a s^b C\gamma_\mu s^c$	1321.71
Σ^{*+}	$\frac{3}{2}^+$	$\frac{1}{\sqrt{3}}(s^a u^b C\gamma_\mu u^c + 2u^a u^b C\gamma_\mu s^c)$	1382.80
Σ^{*0}	$\frac{3}{2}^+$	$\sqrt{\frac{2}{3}}(s^a u^b C\gamma_\mu d^c + u^a d^b C\gamma_\mu s^c + d^a u^b C\gamma_\mu s^c)$	1383.70
Σ^{*-}	$\frac{3}{2}^+$	$\frac{1}{\sqrt{3}}(s^a d^b C\gamma_\mu d^c + 2d^a d^b C\gamma_\mu s^c)$	1387.20
Ξ^{*0}	$\frac{3}{2}^+$	$\frac{1}{\sqrt{3}}(u^a s^b C\gamma_\mu s^c + 2s^a s^b C\gamma_\mu u^c)$	1531.80
Ξ^{*-}	$\frac{3}{2}^+$	$\frac{1}{\sqrt{3}}(d^a s^b C\gamma_\mu s^c + 2s^a s^b C\gamma_\mu d^c)$	1535.00
Ω^-	$\frac{3}{2}^+$	$s^a s^b C\gamma_\mu s^c$	1672.45
Λ_c	$\frac{1}{2}^+$	$c^a u^b C\gamma_5 d^c$	2286.46
Ξ_c^+	$\frac{1}{2}^+$	$c^a u^b C\gamma_5 s^c$	2467.87
Ξ_c^0	$\frac{1}{2}^+$	$c^a d^b C\gamma_5 s^c$	2470.87
$\Xi_c^{'0+}$	$\frac{1}{2}^+$	$\gamma^\mu\gamma^5 c^a u^b C\gamma_\mu s^c$	2577.40
$\Xi_c^{'0}$	$\frac{1}{2}^+$	$\gamma^\mu\gamma^5 c^a d^b C\gamma_\mu s^c$	2578.80
Ω_c	$\frac{1}{2}^+$	$\gamma^\mu\gamma^5 c^a s^b C\gamma_\mu s^c$	2695.20
Ω_c^*	$\frac{3}{2}^+$	$c^a s^b C\gamma_\mu s^c$	2765.90
Λ_b	$\frac{1}{2}^+$	$b^a u^b C\gamma_5 d^c$	5619.40
Ξ_b^0	$\frac{1}{2}^+$	$b^a u^b C\gamma_5 s^c$	5791.90
Ξ_b^-	$\frac{1}{2}^+$	$b^a d^b C\gamma_5 s^c$	5794.50
$\Xi_b^{'0}$	$\frac{1}{2}^+$	$\gamma^\mu\gamma^5 b^a u^b C\gamma_\mu s^c$	5935.02
$\Xi_b^{'-}$	$\frac{1}{2}^+$	$\gamma^\mu\gamma^5 b^a d^b C\gamma_\mu s^c$	5935.02
Ω_b	$\frac{1}{2}^+$	$\gamma^\mu\gamma^5 b^a u^b C\gamma_\mu s^c$	6046.10

VI Model Parameters

Our covariant constituent quark model (CCQM) [21]-[25] contains a number of model parameters which have been determined by a global fit to a multitude of decay processes. The best fit values for the constituent quark masses and the universal infrared cutoff parameter are given by

$$\begin{array}{ccccc}
 m_u & m_s & m_c & m_b & \lambda \\
 \hline
 0.242 & 0.428 & 1.672 & 5.046 & 0.181 \text{ GeV}
 \end{array} \tag{39}$$

The nonlocal quark particle vertices are described in terms of a number of hadronic scale or size parameters Λ_H (in GeV) for which the best fit values are

$$\begin{array}{ccccccc}
 \pi & \eta(\Lambda_{\eta}^{q\bar{q}}, \Lambda_{\eta}^{s\bar{s}}) & \eta'(\Lambda_{\eta'}^{q\bar{q}}, \Lambda_{\eta'}^{s\bar{s}}) & \rho & \omega & \phi & D & D^* \\
 \hline
 0.871 & (0.881, 1.973) & (0.257, 2.797) & 0.610 & 0.490 & 0.880 & 1.600 & 1.530 \\
 \hline
 D_s & D_s^* & B & B^* & B_s & B_s^* & \eta_c & J/\psi \\
 \hline
 1.750 & 1.560 & 1.960 & 1.710 & 2.050 & 1.710 & 2.200 & 1.738 \\
 \hline
 p & \Lambda & \Sigma & \Xi & \Sigma^* & \Xi^* & \Omega & \\
 \hline
 0.3600 & 0.4925 & 0.4925 & 0.4925 & 0.3201 & 0.3201 & 0.3201 & \\
 \hline
 \Lambda_c & \Xi_c & \Omega_c & \Omega_c^* & \Lambda_b & \Xi_b & \Omega_b & \\
 \hline
 0.8675 & 0.8675 & 0.8675 & 0.8675 & 0.5709 & 0.5709 & 0.5709 &
 \end{array} \tag{40}$$

Note, in the case of pseudoscalar mesons we introduce singlet-octet mixing with a mixing angle of $\theta_P = -13.34^\circ$ deduced from Ref. [35] (see details in Refs. [21, 23]) while the vector mesons are assumed to be ideally mixed:

$$\begin{aligned}
 \eta &\longrightarrow -\frac{1}{\sqrt{2}} \sin \delta \Phi_{\Lambda_\eta} (\bar{u}u + \bar{d}d) - \cos \delta \Phi_{\Lambda_{\eta_s}} \bar{s}s, \\
 \eta' &\longrightarrow +\frac{1}{\sqrt{2}} \cos \delta \Phi_{\Lambda_{\eta'}} (\bar{u}u + \bar{d}d) - \sin \delta \Phi_{\Lambda_{\eta'_s}} \bar{s}s, \\
 \delta &= \theta_P - \theta_I, \quad \theta_I = \arctan \frac{1}{\sqrt{2}}.
 \end{aligned} \tag{41}$$

We used [21, 23] the experimental data of the electromagnetic decays involving η and η' to fit the size parameters defining the distribution of nonstrange ($q = u, d$) and strange s quarks in these states: $\Lambda_{\eta}^{q\bar{q}}$, $\Lambda_{\eta'}^{q\bar{q}}$, $\Lambda_{\eta}^{s\bar{s}}$, and $\Lambda_{\eta'}^{s\bar{s}}$.

An important input to the global fit are the mesonic decay constants. Our global fit results in values for the mesonic decay constants which are quite close to the experimental decay constants [36], results of lattice QCD calculations [37, 38] and of nonrelativistic QCD [39] (see Table II).

VII Numerical results

Using the numerical values for the model parameters listed in Sec. VI we present our predictions for the branching ratios, helicity amplitudes, and asymmetry parameters of the nonleptonic decays of single heavy baryons in Tables III-XVI. All nonleptonic decays are described by the generic tree diagram shown in Fig. 3. In our estimate for the branching ratio $\text{Br}(\Lambda_b \rightarrow \Lambda J/\psi) = (8.3 \pm 1.1) \times 10^{-4}$ we used the fragmentation fraction of b quark into Λ baryon of $f_{\Lambda_b} = 7\%$ from [40].

In the future we plan to present predictions also for the nonleptonic modes of heavy baryons which are also contributed to by the W -exchange diagrams. In Ref. [34] we have shown that for some of the heavy-to-light transitions the total contribution of the W -exchange diagrams amount up to approximately 60% of the tree diagram contribution in amplitude, and up to approximately 30% for $b \rightarrow c$ transitions.

TABLE II: Results for the leptonic decay constants f_H (in MeV).

f_H	Our results	Data/Lattice QCD
f_{π^+}	130.3	130.2 ± 1.7 [36]
f_{ρ^+}	218.3	221 ± 1 [36]
f_ω	198.7	198 ± 2 [36]
f_ϕ	226.6	227 ± 2 [36]
f_D	204.7	$203.7 \pm 4.7 \pm 0.6$ [36]
f_{D^*}	244.4	$245 \pm 20^{+3}_{-2}$ [37]
f_{D_s}	256.4	$257.8 \pm 4.1 \pm 0.1$ [36]
$f_{D_s^*}$	272.6	$245 \pm 20^{+3}_{-2}$ [37]
f_{η_c}	426.8	$387 \pm 7 \pm 2$ [38] 346 ± 17 [39]
$f_{J/\psi}$	415.1	416 ± 5 [36]
f_B	192.3	$188 \pm 17 \pm 18$ [36]
f_{B^*}	184.6	$196 \pm 24^{+39}_{-2}$ [37]
f_{B_s}	238.2	227.2 ± 3.4 [36]
$f_{B_s^*}$	217.1	229 ± 46 [37]

1. The decays $\Xi_b^- (\Xi_b^0) \rightarrow \Xi^- (\Xi^0) J/\psi$ and $\Lambda_b \rightarrow \Lambda J/\psi$

The CKM favored decay $\Xi_b^- \rightarrow \Xi^- J/\psi$ was first seen by the CDF [57, 58] and the D0 collaborations [59] in the chain of decays $\Xi_b^- \rightarrow \Xi^- J/\psi$ and $J/\psi \rightarrow \mu^+ \mu^-$, $\Xi^- \rightarrow \Lambda \pi^-$ and $\Lambda \rightarrow p \pi^-$. These measurements led to a first determination of the mass and the lifetime of the Ξ_b^- . PDG 2018 quotes a mass value of 5794.5 ± 1.4 MeV as a weighted average from the two experiments [36]. In a later experiment the LHCb Collaboration collected much higher statistics on the same decay chain [60]. The lifetime of the Ξ_b^- was determined to be $\tau(\Xi_b^-) = 1.571 \pm 0.040$ ps [36]. This is the most accurate determination of the lifetime of the Ξ_b^- to date. Unfortunately a reliable estimate of the branching ratio of the decay $\Xi_b^- \rightarrow \Xi^- J/\psi$ is still missing. The decay $\Xi_b^0 \rightarrow \Xi^0 J/\psi$ is closely related to the decay $\Xi_b^- \rightarrow \Xi^- J/\psi$ by isospin but has not been seen yet.

It is interesting to note that the neutral current transition $\Xi_b^- \rightarrow \Xi^-$ can be related to the neutral current $\Lambda_b \rightarrow \Lambda$ and charged current $\Lambda_b \rightarrow p$ transitions by invoking $SU(3)$ symmetry. This can be seen by using the $\bar{3} \otimes 3 \rightarrow 8$ Clebsch-Gordan table listed in Ref. [61]. Based on the observation that the antisymmetric $[sd]$ and $[ud]$ diquarks are the $(Y = -1/3, I = 1/2)$ and $(Y = 2/3, I = 0)$ members of the $\bar{3}$ multiplet one needs the C.G. coefficients [61].

$$\begin{aligned}
\Xi_b^- \rightarrow \Xi^- : & \quad < \bar{\mathbf{3}}, -\frac{1}{3}, \frac{1}{2}, -\frac{1}{2}; \mathbf{3}, -\frac{2}{3}, 0, 0 | \mathbf{8}, -1, \frac{1}{2}, -\frac{1}{2} > = 1 \\
\Lambda_b \rightarrow \Lambda : & \quad < \bar{\mathbf{3}}, \frac{2}{3}, 0, 0; \mathbf{3}, -\frac{2}{3}, 0, 0 | \mathbf{8}, 0, 0, 0 > = \sqrt{2/3}, \\
\Lambda_b \rightarrow p : & \quad < \bar{\mathbf{3}}, \frac{2}{3}, 0, 0; \mathbf{3}, \frac{1}{3}, \frac{1}{2}, \frac{1}{2} | \mathbf{8}, 1, \frac{1}{2}, \frac{1}{2} > = 1.
\end{aligned} \tag{42}$$

The labeling in (42) proceeds according to the sequence $|\mathbf{R}, Y, I, I_z\rangle$ where \mathbf{R} denotes the relevant $SU(3)$ representation. One does not expect that $SU(3)$ breaking effects are large at the scale of the bottom baryons.

The angular decay distribution for the cascade decay $\Xi_b^- \rightarrow \Xi^- (\rightarrow \Lambda \pi^-) + J/\psi (\rightarrow \ell^+ \ell^-)$ can be adapted from [8] where now one has to use the asymmetry parameter $\alpha_\Xi = -0.458 \pm 0.012$ for the decay $\Xi^- \rightarrow \Lambda \pi^-$ [36]. As in Ref. [8] we introduce the following combinations of helicity amplitudes

$$\begin{aligned}
H_U &= |H_{\frac{1}{2}1}|^2 + |H_{-\frac{1}{2}-1}|^2 && \text{transverse unpolarized,} \\
H_L &= |H_{\frac{1}{2}0}|^2 + |H_{-\frac{1}{2}0}|^2 && \text{longitudinal unpolarized,} \\
H_P &= |H_{\frac{1}{2}1}|^2 - |H_{-\frac{1}{2}-1}|^2 && \text{transverse parity-odd polarized,} \\
H_{L_P} &= |H_{\frac{1}{2}0}|^2 - |H_{-\frac{1}{2}0}|^2 && \text{longitudinal polarized,} \\
H_S &= |H_{\frac{1}{2}t}|^2 + |H_{-\frac{1}{2}t}|^2 && \text{scalar.}
\end{aligned} \tag{43}$$

Following [8, 16, 50] we also introduce linear combinations of normalized squared helicity amplitudes $|\hat{H}_{\lambda_2 \lambda_V}|^2$ by

TABLE III: Branching ratios of nonleptonic two-body decays of heavy baryons (in units of 10^{-4}): $b \rightarrow c$; $c \rightarrow s$ quark-level transition.

Mode	Our results	Data	Theory
$\Lambda_b^0 \rightarrow \Lambda_c^+ D_s^-$	147.8	110 ± 10	230^{+30}_{-40} [41]; 110 [42]; 223 [43]; 77 [44]; 129.1 [45]
$\Lambda_b^0 \rightarrow \Lambda_c^+ D_s^{*-}$	251.6		173^{+20}_{-30} [41]; 91 [42]; 326 [43]; 141.4 [44]; 198.3 [45]
$\Lambda_b^0 \rightarrow \Lambda^0 \eta_c$	4.3		1.5 ± 0.9 [26]
$\Lambda_b^0 \rightarrow \Lambda^0 J/\psi$	8.3	8.3 ± 1.1	1.6 [42]; 2.7 [34]; 6.0 [43]; 2.5 [44]; 2.1 [46]; 3.5 ± 1.8 [47]; 3.3 ± 2.0 [26] 7.8 [28] 8.4 [48]; 8.2 [49]
$\Xi_b^- \rightarrow \Xi^- \eta_c$	1.7		2.3 ± 1.4 [26]
$\Xi_b^0 \rightarrow \Xi^0 \eta_c$	1.6		
$\Xi_b^- \rightarrow \Xi^- J/\psi$	4.6		4.9 ± 3.0 [26]
$\Xi_b^0 \rightarrow \Xi^0 J/\psi$	4.4		
$\Omega_b^- \rightarrow \Omega^- \eta_c$	1.9		
$\Omega_b^- \rightarrow \Omega^- J/\psi$	8.1		

TABLE IV: Branching ratios of nonleptonic two-body decays of heavy baryons (in units of 10^{-4}): $b \rightarrow c$; $u \rightarrow d$ quark-level transition.

Mode	Our results	Theory
$\Omega_b^- \rightarrow \Omega_c^0 \pi^-$	18.8	58.1 [34]
$\Omega_b^- \rightarrow \Omega_c^0 \rho^-$	54.3	
$\Omega_b^- \rightarrow \Omega_c^{*0} \pi^-$	17.0	
$\Omega_b^- \rightarrow \Omega_c^{*0} \rho^-$	55.8	
$\Xi_b^- \rightarrow \Sigma^- D^0$	0.1	
$\Xi_b^- \rightarrow \Sigma^- D^{*0}$	0.3	
$\Omega_b^- \rightarrow \Xi^- D^0$	1.4×10^{-2}	
$\Omega_b^- \rightarrow \Xi^- D^{*0}$	2.6×10^{-2}	
$\Omega_b^- \rightarrow \Xi^{*-} D^0$	0.7×10^{-3}	
$\Omega_b^- \rightarrow \Xi^{*-} D^{*0}$	1.9×10^{-3}	

TABLE V: Branching ratios of nonleptonic two-body decays of heavy baryons (in units of 10^{-4}): $b \rightarrow c$; $c \rightarrow d$ quark-level transition.

Mode	Our results
$\Xi_b^0 \rightarrow \Xi_c^+ D^-$	4.5
$\Xi_b^0 \rightarrow \Xi_c^+ D^{*-}$	9.5
$\Omega_b^- \rightarrow \Omega_c^0 D^-$	2.4
$\Omega_b^- \rightarrow \Omega_c^0 D^{*-}$	3.0
$\Omega_b^- \rightarrow \Omega_c^{*0} D^-$	1.6
$\Omega_b^- \rightarrow \Omega_c^{*0} D^{*-}$	5.8
$\Lambda_b^0 \rightarrow n \eta_c$	0.2
$\Lambda_b^0 \rightarrow n J/\psi$	0.4
$\Xi_b^- \rightarrow \Sigma^- \eta_c$	0.1
$\Xi_b^- \rightarrow \Sigma^- J/\psi$	0.2
$\Xi_b^0 \rightarrow \Lambda^0 \eta_c$	1.6×10^{-2}
$\Xi_b^0 \rightarrow \Sigma^0 \eta_c$	2.9×10^{-2}
$\Xi_b^0 \rightarrow \Lambda^0 J/\psi$	3.1×10^{-2}
$\Xi_b^0 \rightarrow \Sigma^0 J/\psi$	7.0×10^{-2}
$\Omega_b^- \rightarrow \Xi^- \eta_c$	1.3×10^{-2}
$\Omega_b^- \rightarrow \Xi^- J/\psi$	1.8×10^{-2}
$\Omega_b^- \rightarrow \Xi^{*-} \eta_c$	6.9×10^{-2}
$\Omega_b^- \rightarrow \Xi^{*-} J/\psi$	0.2

TABLE VI: Branching ratios of nonleptonic two-body decays of heavy baryons (in units of 10^{-6}): $b \rightarrow c$; $u \rightarrow s$ quark-level transition.

Mode	Our results
$\Xi_b^- \rightarrow \Xi^- D^0$	1.4
$\Xi_b^- \rightarrow \Xi^- D^{*0}$	2.1
$\Omega_b^- \rightarrow \Omega^- D^0$	0.7
$\Omega_b^- \rightarrow \Omega^- D^{*0}$	2.0

TABLE VII: Branching ratios of nonleptonic two-body decays of heavy baryons (in units of 10^{-6}): $b \rightarrow u$; $c \rightarrow s$ quark-level transition.

Mode	Our results	Data	Theory
$\Lambda_b \rightarrow p D_s^-$	13.2	< 480	13.6 [48]; 18 ± 3 [26]
$\Lambda_b \rightarrow p D_s^{*-}$	22.1		6.7 [48]; 8.8 ± 2.2 [26]
$\Omega_b^- \rightarrow \Xi^{*0} D_s^-$	4.9		
$\Omega_b^- \rightarrow \Xi^{*0} D_s^{*-}$	11.3		
$\Omega_b^- \rightarrow \Omega^- \bar{D}^0$	0.1		
$\Omega_b^- \rightarrow \Omega^- \bar{D}^{*0}$	0.3		

TABLE VIII: Branching ratios of nonleptonic two-body decays of heavy baryons (in units of 10^{-8}): $b \rightarrow u$; $u \rightarrow d$ quark-level transition.

Mode	Our results
$\Xi_b^- \rightarrow \Sigma^- \pi^0$	6.2
$\Xi_b^- \rightarrow \Sigma^- \eta$	4.9
$\Xi_b^- \rightarrow \Sigma^- \eta'$	15.2
$\Xi_b^- \rightarrow \Sigma^- \rho^0$	19.0
$\Xi_b^- \rightarrow \Sigma^- \omega$	15.8
$\Omega_b^- \rightarrow \Xi^- \pi^0$	0.5
$\Omega_b^- \rightarrow \Xi^- \eta$	0.4
$\Omega_b^- \rightarrow \Xi^- \eta'$	1.4
$\Omega_b^- \rightarrow \Xi^- \rho^0$	1.7
$\Omega_b^- \rightarrow \Xi^- \omega$	1.4
$\Omega_b^- \rightarrow \Xi^{*-} \pi^0$	2.3
$\Omega_b^- \rightarrow \Xi^{*-} \eta$	2.1
$\Omega_b^- \rightarrow \Xi^{*-} \eta'$	9.5
$\Omega_b^- \rightarrow \Xi^{*-} \rho^0$	257.3
$\Omega_b^- \rightarrow \Xi^{*-} \omega$	213.9

writing

$$\begin{aligned}
\alpha_b &= |\hat{H}_{+\frac{1}{2}0}|^2 - |\hat{H}_{-\frac{1}{2}0}|^2 + |\hat{H}_{-\frac{1}{2}-1}|^2 - |\hat{H}_{+\frac{1}{2}+1}|^2 = \hat{H}_{LP} - \hat{H}_P, \\
r_0 &= |\hat{H}_{+\frac{1}{2}0}|^2 + |\hat{H}_{-\frac{1}{2}0}|^2 = \hat{H}_L, \\
r_1 &= |\hat{H}_{+\frac{1}{2}0}|^2 - |\hat{H}_{-\frac{1}{2}0}|^2 = \hat{H}_{LP},
\end{aligned} \tag{44}$$

where $|\hat{H}_{\lambda_2 \lambda_V}|^2 = |H_{\lambda_2 \lambda_V}|^2 / \mathcal{H}_N$ and where the normalization factor \mathcal{H}_N is given by

$$\mathcal{H}_N \equiv |H_{+\frac{1}{2}0}|^2 + |H_{-\frac{1}{2}0}|^2 + |H_{-\frac{1}{2}-1}|^2 + |H_{+\frac{1}{2}+1}|^2. \tag{45}$$

The full joint angular decay distribution of the cascade decay $B_1 \rightarrow B_2(\rightarrow B_3 + P) + V(\rightarrow \ell^+ \ell^-)$ including the polarization of the parent baryon and including lepton mass effects has been given in [8]. The angular decay

TABLE IX: Branching ratios of nonleptonic two-body decays of heavy baryons (in units of 10^{-8}): $b \rightarrow u$; $c \rightarrow d$ quark-level transition.

Mode	Our results
$\Xi_b^0 \rightarrow \Sigma^+ D^-$	13.6
$\Xi_b^0 \rightarrow \Sigma^+ D^{*-}$	29.6
$\Xi_b^- \rightarrow \Sigma^0 D^-$	7.2
$\Xi_b^- \rightarrow \Sigma^0 D^{*-}$	15.6
$\Omega_b^- \rightarrow \Xi^0 D^-$	1.6
$\Omega_b^- \rightarrow \Xi^0 D^{*-}$	2.6
$\Omega_b^- \rightarrow \Xi^{*0} D^-$	6.7
$\Omega_b^- \rightarrow \Xi^{*0} D^{*-}$	18.5
$\Omega_b^- \rightarrow \Xi^- \bar{D}^0$	7.3×10^{-2}
$\Omega_b^- \rightarrow \Xi^- \bar{D}^{*0}$	13.2×10^{-2}
$\Omega_b^- \rightarrow \Xi^{*-} \bar{D}^0$	6.8
$\Omega_b^- \rightarrow \Xi^{*-} \bar{D}^{*0}$	18.9

TABLE X: Branching ratios of nonleptonic two-body decays of heavy baryons (in units of 10^{-9}): $b \rightarrow u$; $u \rightarrow s$ quark-level transition.

Mode	Our results
$\Xi_b^- \rightarrow \Xi^- \pi^0$	0.8
$\Xi_b^- \rightarrow \Xi^- \eta$	0.5
$\Xi_b^- \rightarrow \Xi^- \eta'$	1.3
$\Xi_b^- \rightarrow \Xi^- \rho^0$	2.8
$\Xi_b^- \rightarrow \Xi^- \omega$	2.1
$\Omega_b^- \rightarrow \Omega^- \pi^0$	0.7
$\Omega_b^- \rightarrow \Omega^- \eta$	0.5
$\Omega_b^- \rightarrow \Omega^- \eta'$	1.1
$\Omega_b^- \rightarrow \Omega^- \rho^0$	9.1
$\Omega_b^- \rightarrow \Omega^- \omega$	7.6

TABLE XI: Branching ratios of nonleptonic two-body decays of heavy baryons (in units of 10^{-2}): $c \rightarrow s$; $d \rightarrow u$ quark-level transition.

Mode	Our results	Theory
$\Xi_c^+ \rightarrow \Xi^{*0} \pi^+$	8.1×10^{-6}	
$\Xi_c^+ \rightarrow \Xi^{*0} \rho^+$	3.9×10^{-6}	
$\Omega_c^0 \rightarrow \Omega^- \pi^+$	0.2	1.0 [42]
$\Omega_c^0 \rightarrow \Omega^- \rho^+$	1.9	3.6 [42]
$\Omega_c^0 \rightarrow \Xi^{*0} \bar{K}^0$	0.3	
$\Omega_c^0 \rightarrow \Xi^{*0} \bar{K}^{*0}$	2.0	

distribution involves the longitudinal and transverse polarization components for the daughter baryon B_2 defined by

$$\begin{aligned}
 P_z(B_2) &= |\hat{H}_{+\frac{1}{2}0}|^2 - |\hat{H}_{-\frac{1}{2}0}|^2 + |\hat{H}_{+\frac{1}{2}+1}|^2 - |\hat{H}_{-\frac{1}{2}-1}|^2 = \hat{H}_{L_P} + \hat{H}_P, \\
 P_x(B_2) &= 2 \operatorname{Re} \left(\hat{H}_{\frac{1}{2}1} \hat{H}_{-\frac{1}{2}0}^* + \hat{H}_{\frac{1}{2}0} \hat{H}_{-\frac{1}{2}-1}^* \right).
 \end{aligned} \tag{46}$$

Note that one can express the longitudinal polarization of the daughter baryon in terms of the linear combinations r_1 and α_b in (44), i.e. one has $P_z(B_2) = 2r_1 - \alpha_b = \hat{H}_{L_P} + \hat{H}_P$. The magnitude of the transverse polarization $P_x(B_2)$ determines the size of the azimuthal correlations between the baryon-side and lepton-side decay plains.

Instead of listing the full angular decay distribution including azimuthal terms we shall only list the two-fold polar

angle decay distribution given by

$$W(\theta_3, \theta_\ell) = \frac{1}{4} \left(1 + P_z(B_2) \alpha_{B_2} \cos \theta_3 \right) v \cdot (1 + 2\varepsilon) + \frac{1}{4} \left((1 - 3r_0)(3 \cos^2 \theta_\ell - 1) - (\alpha_b + r_1) \alpha_{B_2} (3 \cos^2 \theta_\ell - 1) \cos \theta_3 \right) v \cdot v^2 \quad (47)$$

α_{B_2} denotes the asymmetry factor in the decay $B_2 \rightarrow B_3 + P$, a quantity known from experiment in many cases. One can reexpress the two angular parameters $(1 - 3r_0)$ and $(\alpha_b + r_1)$ in (47) through the components \hat{H}_I by writing $(1 - 3r_0) = (\hat{H}_U - 2\hat{H}_L)$ and $(\alpha_b + r_1) = (2\hat{H}_{LP} - \hat{H}_P)$. Note that we have kept the overall lepton velocity factor $v = \sqrt{1 - 4m_\ell^2/q^2}$ in (47) which results from the momentum factor in the decay formula for $V \rightarrow \ell^+ \ell^-$. The trigonometric function $(3 \cos^2 \theta_\ell - 1)$ appearing in Eq. (47) integrates to zero upon $\cos^2 \theta_\ell$ integration. In the literature one frequently finds $(3 \cos^2 \theta_\ell - 1) = 2 P_2(\cos \theta_\ell)$ written in terms of the Legendre polynomial $P_2(\cos \theta_\ell)$ of second degree.

We define partial helicity widths in terms of the following bilinear helicity expressions

$$\Gamma_I = \frac{G_F^2}{32\pi} \frac{|\mathbf{p}_2|}{M_1^2} |V_{ij} V_{kl}^\dagger|^2 C_{\text{eff}}^2 f_V^2 M_V^2 H_I, \quad I = U, L, P, LP. \quad (48)$$

The total $B_1 \rightarrow B_2 V$ decay width is given by

$$\Gamma(B_1 \rightarrow B_2 V) = \Gamma_U + \Gamma_L. \quad (49)$$

We shall also be interested in the cascade decays $B_1 \rightarrow B_2(\rightarrow B_3 P) + V(\rightarrow P P)$ as, e.g., in $\Lambda_b \rightarrow \Lambda_c(\rightarrow p \bar{K}^0) + D_s^*(\rightarrow D \pi)$. The two-fold polar angle distribution can be calculated to be

$$4W(\theta_3, \theta_P) = (1 + P_z(B_2) \alpha_{B_2} \cos \theta_3 + (\hat{H}_U + \frac{1}{2} \hat{H}_L)(3 \cos^2 \theta_P - 1) + (\hat{H}_{LP} + \frac{1}{2} \hat{H}_P) \alpha_{B_2} \cos \theta_3 (3 \cos^2 \theta_P - 1)) \quad (50)$$

Moduli squared of normalized helicity amplitudes and asymmetry parameters for the cascade decay $\Lambda_b \rightarrow \Lambda_c(\rightarrow p \bar{K}^0) + D_s^*(\rightarrow D \pi)$ are shown in Table XII.

TABLE XII: Moduli squared of normalized helicity amplitudes and asymmetry parameters for the cascade decay $\Lambda_b \rightarrow \Lambda_c(\rightarrow p \bar{K}^0) + D_s^*(\rightarrow D \pi)$ transition.

Quantity	Our results	Quantity	Our results	Quantity	Our results
$ \hat{H}_{+\frac{1}{2}+1} ^2$	4.46×10^{-2}	\hat{H}_U	0.358	α_b	-0.364
$ \hat{H}_{+\frac{1}{2}0} ^2$	4.98×10^{-3}	\hat{H}_L	0.642	r_0	0.642
$ \hat{H}_{-\frac{1}{2}0} ^2$	0.637	\hat{H}_P	-0.268	r_1	-0.632
$ \hat{H}_{-\frac{1}{2}-1} ^2$	0.313	\hat{H}_{LP}	-0.633	(P_x, P_z)	(-0.901, 0.416)

Next we turn to the decay $\Lambda_b \rightarrow \Lambda J/\psi$. The angular decay distribution of the cascade chain $\Lambda_b \rightarrow \Lambda(\rightarrow p \pi^-) + J/\psi(\rightarrow \ell^+ \ell^-)$ including polarization effects of the parent baryon Λ_b has been discussed in detail in [15, 16, 25]. A new insight has been gained concerning the accessibility of the polarization of the produced parent baryon Λ_b [51]. In a symmetric collider such as the pp -collider where the sample of Λ_b 's are produced over a symmetric interval of pseudorapidity the polarization of the Λ_b must average to zero. In order to access the polarization of the Λ_b one must e.g. divide the pseudorapidity interval into two forward and backward hemispheres which has not been done in the LHCb [50] and ATLAS [51] experiments. We shall therefore no longer discuss the polarization dependent terms in the angular decay distribution. Such a measurement has to wait for a future analysis.

We list some numerical results of our previous analysis on the decay $\Lambda_b \rightarrow \Lambda J/\psi$ in Table XIII. Table XIII shows that the longitudinal polarization of the daughter baryon Λ is almost 100 % and negative. In fact, one finds $P_z(\Lambda) = \hat{H}_{LP} + \hat{H}_P = -0.995$. This leaves very little room for the transverse polarization $P_x(\Lambda)$ since $P_z^2(\Lambda) + P_x^2(\Lambda) = 1$. We set the T -odd polarization component $P_x(\Lambda)$ to zero since the helicity amplitudes are nearly real in our analysis. From the numbers in Table XIII and using the definition (46) one finds $P_x(\Lambda) = 0.095$. A small transverse polarization $P_x(\Lambda)$ in turn implies small azimuthal correlations between the two planes defined by (p, π^-) and (ℓ^+, ℓ^-) as was found in [8] and which has been confirmed by the azimuthal measurement in [51].

For the asymmetry parameter α_b we obtained the small negative value $\alpha_b \simeq -0.07$ [25]. The value of α_b determines the analyzing power of the cascade decay $\Lambda_b \rightarrow \Lambda(\rightarrow p \pi^-) + J/\psi(\rightarrow \ell^+ \ell^-)$ to measure the polarization of the parent baryon Λ_b . A small value of α_b implies a poor analyzing power of such an experiment. Our calculated value

TABLE XIII: Moduli squared of normalized helicity amplitudes and asymmetry parameters for the $\Lambda_b \rightarrow \Lambda(\rightarrow p \pi^-) J/\psi(\rightarrow \ell^+ \ell^-)$ transition.

Quantity	Our results	LHCb [50]	ATLAS [51]	CMS [52]
$ \widehat{H}_{+\frac{1}{2}+1} ^2$	2.34×10^{-3}	$-0.10 \pm 0.04 \pm 0.03$	$(0.08^{+0.13}_{-0.08} \pm 0.06)^2$	$0.05 \pm 0.04 \pm 0.02$
$ \widehat{H}_{+\frac{1}{2}0} ^2$	3.24×10^{-4}	$0.01 \pm 0.04 \pm 0.03$	$(0.17^{+0.12}_{-0.17} \pm 0.09)^2$	$-0.02 \pm 0.03 \pm 0.02$
$ \widehat{H}_{-\frac{1}{2}0} ^2$	0.532	$0.57 \pm 0.06 \pm 0.03$	$(0.59^{+0.06}_{-0.07} \pm 0.03)^2$	$0.51 \pm 0.03 \pm 0.02$
$ \widehat{H}_{-\frac{1}{2}-1} ^2$	0.465	$0.51 \pm 0.05 \pm 0.02$	$(0.79^{+0.04}_{-0.05} \pm 0.02)^2$	$0.46 \pm 0.02 \pm 0.02$
α_b	-0.069	$0.05 \pm 0.17 \pm 0.07$	$0.30 \pm 0.16 \pm 0.06$	$-0.12 \pm 0.13 \pm 0.06$
r_0	0.533	$0.58 \pm 0.02 \pm 0.01$		
r_1	-0.532	$-0.56 \pm 0.10 \pm 0.05$		
$P_z(\Lambda)$	-0.995	$-1.17 \pm 0.26 \pm 0.12$		
$P_x(\Lambda)$	0.095			

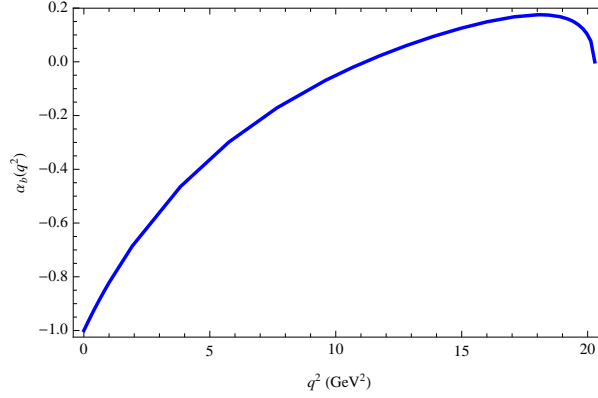


FIG. 4: q^2 dependence of the asymmetry parameter $\alpha_b(q^2)$ in the $\Lambda_b \rightarrow \Lambda$ transition.

for the asymmetry parameter $\alpha_b = -0.07$ agrees within one standard deviation with the slightly revised value of the asymmetry parameter $\alpha_b = 0.05 \pm 0.17 \pm 0.07$ reported in [50]. A new measurement on α_b was reported by the ATLAS collaboration [51]. Our result is more than two standard deviations away from their reported value of $\alpha_b = 0.30 \pm 0.16 \pm 0.06$. We mention that most of the theoretical model calculations predict small negative values for α_b ranging from (-0.09) to (-0.21) (see Table VI in [8]) except the calculation of [62, 63] who quote a value of $\alpha_b = 0.777$. We believe the calculation of [62, 63] to be erroneous. The relation between the helicity amplitudes and the HQET form factors F_1 and F_2 given in [62, 63] is not correct. They also obtain a polarization of the daughter baryon Λ of $P_z(\Lambda) = -9\%$ which is much smaller than what is obtained in the other model calculations.

In Fig. 4 we show a plot of α_b over the whole range of accessible q^2 -values. At the kinematical limits $q^2 = 0$ and $q^2 = (M_1 - M_2)^2 = 20.28 \text{ GeV}^2$ α_b takes the values $\alpha_b = -1$ and $\alpha_b = 0$ in agreement with the corresponding limiting values of Eq. (44). The asymmetry parameter α_b goes through zero between $q^2 = m_{J/\psi}^2 = 9.59 \text{ GeV}^2$ and $q^2 = m_{\psi(2S)}^2 = 13.59 \text{ GeV}^2$ as demonstrated in the numerical results of [25]. We show this plot in order to demonstrate that it is very unlikely that the asymmetry value reaches a large positive value as in [62, 63] between the above two model independent limiting values.

2. The decays $\Lambda_b^0 \rightarrow \Lambda_c^+ D_s^-$ and $\Lambda_b^0 \rightarrow \Lambda_c^+ D^-$

Both the Cabibbo-favored decay $\Lambda_b^0 \rightarrow \Lambda_c^+ D_s^-$ and the Cabibbo suppressed decay $\Lambda_b^0 \rightarrow \Lambda_c^+ D^-$ have been seen by the LHCb collaboration [64]. The PDG 2018 quotes branching fractions of $\mathcal{B}(\Lambda_b^0 \rightarrow \Lambda_c^+ D_s^-) = (1.1 \pm 0.1) \times 10^{-2}$ and $\mathcal{B}(\Lambda_b^0 \rightarrow \Lambda_c^+ D^-) = (4.6 \pm 0.6) \times 10^{-4}$ for these decays [36].

We employ a notation where we label the scalar time component of the current by the suffix " t " where $\lambda_t = 0$ in order to distinguish between the ($J = 0$) and ($J = 1$) transformation of the two helicity zero cases. We shall again define normalized helicity amplitudes by writing $|\widehat{H}_{\lambda_2 t}|^2 = |H_{\lambda_2 t}|^2 / \mathcal{H}_N$ where \mathcal{H}_N is now given by $\mathcal{H}_N = |H_{\frac{1}{2}t}|^2 + |H_{-\frac{1}{2}t}|^2$.

In this notation the longitudinal polarization of the daughter baryon B_2 is given by

$$P_z(B_2) = |\hat{H}_{\frac{1}{2}t}|^2 - |\hat{H}_{-\frac{1}{2}t}|^2 = \begin{cases} -0.989, & \Lambda_b \rightarrow \Lambda_c D \text{ mode} \\ -0.986, & \Lambda_b \rightarrow \Lambda_c D_s \text{ mode} \end{cases} \quad (51)$$

One then has the polar decay distribution

$$W(\theta_3) \propto (1 + P_z(B_2)\lambda_{B_2} \cos \theta_3) . \quad (52)$$

The transverse polarization component $P_x(B_2)$ does not come into play in these decays.

3. The $1/2^+ \rightarrow 3/2^+ + 1^-$ factorizing decay $\Omega_b^- \rightarrow \Omega^- J/\psi$

The Ω_b^- has a clear signature through the decay $\Omega_b^- \rightarrow \Omega^- J/\psi$. This decay mode was first observed in [58, 65]. The PDG 2018 quotes the average values for the mass 6046.1 ± 1.7 MeV and the life time $\tau(\Omega_b^-) = 1.65_{-0.16}^{+0.18}$ ps [60]. We shall take the LHCb result for our evaluation of branching rates.

We begin with the decay $1/2^+ \rightarrow 3/2^+ 1^-$ where we concentrate on the decay chains of the daughter baryon $3/2^+ \rightarrow 1/2^+ + P$ and the vector meson $V \rightarrow \ell^+ \ell^-$.

TABLE XIV: Moduli squared of normalized helicity amplitudes and asymmetry parameters for the cascade decay $\Omega_b \rightarrow \Omega^- (\rightarrow \Xi^- p, \Lambda K^-) + J/\psi (\rightarrow \ell^+ \ell^-)$ transitions.

Quantity	Our results
$\mathcal{B}(\Omega_b \rightarrow \Omega^- J/\psi)$	0.08 %
$\hat{\mathcal{H}}_{U_{1/2}}$	0.236
$\hat{\mathcal{H}}_{U_{3/2}}$	0.312
$\hat{\mathcal{H}}_L$	0.452

In Table XIV we list our results on the branching ratio of this decay together with our values for $\hat{\mathcal{H}}_{U_{1/2}}$, $\hat{\mathcal{H}}_{U_{3/2}}$ and $\hat{\mathcal{H}}_L$. Latter values determine the polar angle distribution of the subsequent decay $\Omega^- \rightarrow \Xi \pi, \Lambda K^-$. We have defined $\hat{\mathcal{H}}_{U_{1/2}} = |\hat{H}_{\frac{1}{2}1}|^2 + |\hat{H}_{-\frac{1}{2}-1}|^2$, $\hat{\mathcal{H}}_{U_{3/2}} = |\hat{H}_{\frac{3}{2}1}|^2 + |\hat{H}_{-\frac{3}{2}-1}|^2$ and $\hat{\mathcal{H}}_L = |\hat{H}_{\frac{1}{2}0}|^2 + |\hat{H}_{-\frac{1}{2}0}|^2$, where, as before, $|\hat{H}_{\lambda_2 \lambda_V}|^2 = |H_{\lambda_2 \lambda_V}|^2 / \mathcal{H}_V$ and $\mathcal{H}_V = \sum_{\lambda_2, \lambda_V} |H_{\lambda_2 \lambda_V}|^2$. A much smaller value of the branching fraction has been calculated in [28] where the authors predict $\mathcal{B}(\Omega_b \rightarrow \Omega^- J/\psi) = 4.5 \times 10^{-5}$. The smallness of the branching ratio in the calculation [28] can be traced to the erroneous assumption that the transition form factors in the process fall from $q^2 = 0$ to $q^2 = m_{J/\psi}^2$.

We define partial helicity widths in terms of the following bilinear helicity expressions

$$\Gamma_I = \frac{G_F^2}{32\pi} \frac{|\mathbf{p}_2|}{M_1^2} |V_{ij} V_{kl}^*|^2 C_{\text{eff}}^2 f_V^2 M_V^2 \mathcal{H}_I, \quad I = U_{1/2}, U_{3/2}, L. \quad (53)$$

The $B_1 \rightarrow B_2 V$ decay width is given by

$$\Gamma(B_1(1/2^+) \rightarrow B_2(3/2^+) V) = \Gamma_{U_{1/2}} + \Gamma_{U_{3/2}} + \Gamma_L. \quad (54)$$

The two-fold joint angular decay distribution for the cascade decay $1/2^+ \rightarrow 3/2^+ (\rightarrow 1/2^+ 0^-) + V (\rightarrow \ell^+ \ell^-)$ is simplified by the observation that the relevant decays of the daughter baryon with $B_2(3/2^+) \rightarrow B_3(1/2^+) 0^-$ and $\Omega^- \rightarrow \Xi \pi, \Lambda K^-$ are almost purely parity conserving [36], i.e. for the decay $3/2^+ \rightarrow 1/2^+ 0^-$ one has $H_{\lambda_3 0} = H_{-\lambda_3 0}$. This also follows from a simple quark model calculation [54, 66]. The fact that the vector current induced transition $3/2^+ \rightarrow 1/2^+$ is conserved in the simple quark model can be traced to the approximation that there is no spin interaction between the two light spectator quarks [67]. This means there will be no parity-odd linear $\cos \theta_{B_3}$ terms in the angular decay distribution.

The two-fold joint polar angle decay distribution can be derived from the master formula

$$W(\theta_\ell, \theta_B) \propto \sum_{\text{helicities}} |h_{\lambda_{\ell^+} \lambda_{\ell^-}}^V|^2 \left[d_{\lambda_V, \lambda_{\ell^+} - \lambda_{\ell^-}}^1(\theta_\ell) \right]^2 |H_{\lambda_2 \lambda_V}|^2 \left[d_{\lambda_2 \lambda_3}^{3/2}(\theta_B) \right]^2, \quad (55)$$

where the summation extends over all possible helicities $\lambda_{\ell^+}, \lambda_{\ell^-}, \lambda_2, \lambda_3 = \pm \frac{1}{2}$ and $\lambda_V = 0, \pm 1$. In (55) we have left out the overall factor $|H_{\lambda_3 0}|^2$. The required table of the Wigner symbol $d_{mm'}^{3/2}(\theta)$ can be found e.g. in [68].

The vector current leptonic helicity amplitudes for the decay $V \rightarrow \ell^+ \ell^-$ are given by (see [25])

$$\text{flip: } h_{-\frac{1}{2}-\frac{1}{2}}^V = h_{+\frac{1}{2}+\frac{1}{2}}^V = 2m_l, \quad \text{nonflip: } h_{-\frac{1}{2}+\frac{1}{2}}^V = h_{+\frac{1}{2}-\frac{1}{2}}^V = \sqrt{2q^2}. \quad (56)$$

For the angular decay distribution one obtains

$$\begin{aligned} W(\theta_{B_3}, \theta_\ell) \propto & \frac{3}{8} v \left((1 + \cos^2 \theta_\ell) v + 8\varepsilon \right) \frac{1}{4} \left(\hat{\mathcal{H}}_{U_{1/2}} (1 + 3 \cos^2 \theta_{B_3}) + \hat{\mathcal{H}}_{U_{3/2}} 3 \sin^2 \theta_{B_3} \right) \\ & + \hat{\mathcal{H}}_L \frac{3}{8} v \left((1 + \cos^2 \theta_\ell) v + 8\varepsilon \right) \frac{1}{4} (1 + 3 \cos^2 \theta_{B_3}) \end{aligned} \quad (57)$$

We have again included an overall factor of $v = (1 - 4\varepsilon)^{1/2}$ from the momentum factor in the decay formula for the decay $V \rightarrow \ell^+ \ell^-$.

As in Eq. (47) we can represent the angular decay distribution in an equivalent form in terms of the second order Legendre polynomials $P_2(x) = (3x^2 - 1)/2$ with $x = \cos \theta_{B_3}, \cos \theta_\ell$. Using the same normalization as in (57) one has

$$\begin{aligned} 4W(\theta_{B_3}, \theta_\ell) \propto & v(1 + 2\varepsilon) + \frac{1}{2}(3 \cos^2 \theta_{B_3} - 1) \left(\hat{\mathcal{H}}_{U_{1/2}} - \hat{\mathcal{H}}_{U_{3/2}} + \hat{\mathcal{H}}_L \right) v(1 + 2\varepsilon) + \frac{1}{4}(3 \cos^2 \theta_\ell - 1) v^3 \\ & + \frac{1}{8}(3 \cos^2 \theta_{B_3} - 1)(3 \cos^2 \theta_\ell - 1) \left(\mathcal{H}_{U_{1/2}} - \hat{\mathcal{H}}_{U_{3/2}} + \hat{\mathcal{H}}_L \right) v^3 \end{aligned} \quad (58)$$

such that the angle dependent parts integrates to zero [16]. Upon integration one has

$$\int d \cos \theta_\ell d \cos \theta_B W(\theta_B, \theta_\ell) = \left(\hat{\mathcal{H}}_{U_{1/2}} + \hat{\mathcal{H}}_{U_{3/2}} + \hat{\mathcal{H}}_L \right) v(1 + 2\varepsilon) = v(1 + 2\varepsilon). \quad (59)$$

Next we discuss the decays $1/2^+ \rightarrow 3/2^+ 0^-$. Similar to the current induced transition $3/2^+ \rightarrow 1/2^+$ one finds from a naive quark model calculation [54] that the vector current transition $\langle 3/2^+ | J_\mu^V | 1/2^+ \rangle$ is conserved. The basic mechanism is the same as mentioned in the discussion of the $\langle 1/2^+ | J_\mu^V | 3/2^+ \rangle$ transition. The crucial assumption is that there is no spin interaction between the spectator quarks. The conservation of the vector current implies that the helicity amplitudes $H_{\pm\lambda_2, t}^V$ vanish, i.e. one has $H_{\pm\lambda_2, t}^V = 0$. We also find vector current conservation $q^\mu \langle 3/2^+ | J_\mu^V | 1/2^+ \rangle = 0$ in our more sophisticated CCQM quark model, i.e. one has again $H_{\pm\lambda_2, t}^V = 0$. The vector current conservation in the CCQM can be traced to the structure of the interpolating currents of the Ω_c and Ω^- of Table I.

The rate can be calculated from

$$\Gamma(1/2^+ \rightarrow 3/2^+ 0^-) = \frac{G_F^2}{32\pi} \frac{|\mathbf{p}_2|}{M_1^2} |V_{ij} V_{kl}^\dagger|^2 C_{\text{eff}}^2 f_P^2 M_P^2 \mathcal{H}_S, \quad (60)$$

where $\mathcal{H}_S = |H_{\frac{1}{2}t}|^2 + |H_{-\frac{1}{2}t}|^2 = 2|H_{\frac{1}{2}t}|^2$. The corresponding branching ratio for $\Omega_b^- \rightarrow \Omega^- \eta_c$ is predicted to be $\mathcal{B} = 5.0 \times 10^{-4}$ (see Table III).

The baryon-side decay distribution in this decay is identical to that of the longitudinal contribution in Eq. (57), i.e. one has

$$W(\theta_{B_3}) = \frac{1}{4}(1 + 3 \cos \theta_{B_3}) = \frac{1}{2}(1 + \frac{1}{2}(3 \cos \theta_{B_3} - 1)) = \frac{1}{2}(1 + P_2(\cos \theta_{B_3})). \quad (61)$$

4. The decay $\Lambda_c \rightarrow p + \phi$

The Cabibbo-suppressed charm baryon decay $\Lambda_c \rightarrow p\phi$ was first observed by the ACCMOR Collaboration in the NA32 experiment at CERN [69] with a branching ratio of $B(\Lambda_c \rightarrow p\phi)/B(\Lambda_c \rightarrow pK^-\pi^+) = 0.04 \pm 0.03$. Three years later the E687 Collaboration at Fermilab reported an upper limit for its branching relative to the mode $B(\Lambda_c \rightarrow p\phi)/B(\Lambda_c \rightarrow pK^-K^+) < 0.58$ at 90% C.L. [70]. In 1996 the CLEO Collaboration [71] confirmed the previously observed $\Lambda_c \rightarrow p\phi$ decay mode with significant statistics and measured the branching ratios $B(\Lambda_c \rightarrow p\phi)/B(\Lambda_c \rightarrow pK^-\pi^+) = 0.024 \pm 0.006 \pm 0.003$ and $B(\Lambda_c \rightarrow p\phi)/B(\Lambda_c \rightarrow pK^-K^+) = 0.62 \pm 0.20 \pm 0.12$. Finally, in 2002 the Belle Collaboration at KEK [72] measured the ratio of branching rates with much higher accuracy $B(\Lambda_c \rightarrow p\phi)/B(\Lambda_c \rightarrow pK^-\pi^+) = 0.015 \pm 0.002 \pm 0.002$.

The good news is that the long-standing problem of the absolute branching ratio of the decay $\Lambda_c \rightarrow pK^-\pi^+$ has been solved by the BELLE [73] and the BES III collaborations [74]. Thus the above branching rate ratios can be converted into absolute branching ratios.

In the present case the information on the polarization of the daughter baryon, the proton, is of no particular interest since the polarization of the proton cannot be probed. The angular decay distribution on the lepton side can be read off from Table I in Ref. [8] or can be obtained by integrating Eq. (47) over $\cos\theta_3$. One has ($\varepsilon = m_\ell^2/m_\phi^2$)

$$W(\theta_\ell) \propto v(1+2\varepsilon) \left(1 + \frac{1}{4} \frac{v^2}{1+2\varepsilon} (\hat{H}_U - 2\hat{H}_L)(3\cos^2\theta_\ell - 1) \right) \quad (62)$$

where θ_ℓ is the polar angle of either of the leptons with respect to the momentum direction of the ϕ in the Λ_c rest frame. Note that the second $\cos\theta_\ell$ -dependent term vanishes after integration. The muon mass corrections to the rate term in (62) are quite small as is evident from the expansion $v(1+2\varepsilon) = 1 - 4\varepsilon^2 + O(\varepsilon^3) \approx 0.998$. The muon mass corrections to the $\cos\theta_\ell$ dependent term, however, are larger and can be seen to amount to $v^2/(1+2\varepsilon) = 1 - 6\varepsilon + O(\varepsilon^3) \simeq 6\%$.

We present our results in Tables XV and XVI and compare them with data presented by the Particle Data Group [36] and the predictions of other theoretical approaches [34, 53–56]. We calculate the width of the cascade decay $\Lambda_c \rightarrow p + \phi(\rightarrow \ell^+\ell^-)$ by using the zero width approximation

$$B(\Lambda_c \rightarrow p + \phi(\rightarrow \ell^+\ell^-)) = B(\Lambda_c \rightarrow p + \phi) B(\phi \rightarrow \ell^+\ell^-). \quad (63)$$

We take the value of the leptonic decay constant $f_\phi = 226.6$ MeV from the e^+e^- mode calculated in our approach in agreement with data. Using the result Eq. (62) we can write down the general $m_\ell \neq 0$ decay formula

$$\Gamma(\phi \rightarrow \ell^+\ell^-) = \frac{4\pi\alpha^2}{27} \frac{f_\phi^2}{m_\phi} \sqrt{1 - \frac{4m_\ell^2}{m_\phi^2}} \left(1 + \frac{2m_\ell^2}{m_\phi^2} \right) \quad (64)$$

to evaluate the muonic mode. As already remarked above, muon mass effects are negligible in the rate as Table XVI shows. Note that we give more stringent upper limits on the branching ratios of these decays compared to the data [36]. The numerical value for the asymmetry ($\hat{H}_U - 2\hat{H}_L$) is

$$\hat{H}_U - 2\hat{H}_L = -0.735. \quad (65)$$

TABLE XV: Branching ratio $B(\Lambda_c \rightarrow p\phi)$ in units 10^{-4} .

Our result	Theoretical predictions	Data [36]
14.0	19.5 [53]; 21.5 [54]; 9.89 [55]; 4.0 [56]; 27.3 ± 17.9 [34]	10.8 ± 1.4

TABLE XVI: Branching ratios $B(\Lambda_c \rightarrow p\phi(\ell^+\ell^-))$ in units of 10^{-7} .

Mode	Our results	Data [36]
$\Lambda_c \rightarrow p + e^+e^-$	4.11	< 55
$\Lambda_c \rightarrow p + \mu^+\mu^-$	4.11	< 440

VIII Summary

We have calculated the decay properties of a number of nonleptonic heavy baryon decays. Of the many possible nonleptonic heavy baryon decays we have singled out those decays which proceed solely through the tree diagram contribution without a possible contamination from W -exchange contributions. Note that we have not included penguin-type operators in our set of operators as, e.g., the penguin operator governing the quark-level transition $b \rightarrow s\bar{s}s$ that induces the decay $\Lambda_b \rightarrow \Lambda + \phi$ recently seen by the LHCb Collaboration [75]. We plan to study decays induced by penguin-type operators in the future. For the decays dominated by tree diagram contribution we have calculated decay rates, branching ratios and asymmetry parameters associated with the polar angle distributions of their subsequent decay chains. Some of these decays have been seen which has lead to measurements of their lifetimes and their masses. We have also provided results for decays with prominent branching ratios and signatures which have not been observed up to now. Measuring lifetimes and masses is only the first step towards a comprehensive analysis

of heavy baryon decays which would aim for the determination of branching ratios and asymmetry parameters in angular decay distributions as has e.g. been done in the decay $\Lambda_b \rightarrow \Lambda J/\psi$. We estimate our errors on branching fractions to be $\sim 20\%$. Our errors on the asymmetry parameters are much smaller since the errors cancel out in the helicity rate ratios that describe the asymmetry parameters.

It would be interesting to extend our analysis to all nonleptonic two-body decays of the heavy baryons. Such a calculation would involve also contributions from the W -exchange graphs called color commensurate (C), exchange (E) and bow-tie (B) graphs in [1]. For the decays of the bottom baryon states the authors of [1] derived a hierarchy of strength $T \gg C, E \gg B$ from a qualitative SCET analysis. It would be interesting to find out whether the dominance of the tree graph contribution in the $b \rightarrow c$ and $b \rightarrow u$ sector predicted in [1] is borne out by the phenomenology of these decays. In particular, it would be interesting to determine the size of the W -exchange contributions to the decays $\Lambda_b \rightarrow \Lambda \eta(\eta')$. Within the general class of nonleptonic two-body baryon decays one also finds decays which proceed solely by W -exchange diagrams. Among these are the decays in which the transition between the two spectator quarks is forbidden due to the fact that one has a transition between a symmetric and antisymmetric spin-flavor configuration such as in $[ud] \rightarrow \{ud\}$. A few examples are the $c \rightarrow s\bar{d}u$ decays $\Lambda_c^+ \rightarrow \Delta^{++}K^-$, $\Lambda_c^+ \rightarrow \Sigma^0\pi^+$ and $\Xi_c^0 \rightarrow \Omega^-K^+$. Then there is a multitude of decays where the flavor composition of the parent and daughter baryon preclude a tree graph contribution. In the $(c \rightarrow s; d \rightarrow u)$ sector two sample decays are $\Lambda_c^+ \rightarrow \Xi^0 K^+$ and $\Lambda_c^+ \rightarrow \Xi^{*0}(1530) K^+$ which have been observed with the sizable branching ratios of $\mathcal{B} = (5.90 \pm 0.86 \pm 0.39) \times 10^{-3}$ and $\mathcal{B} = (5.02 \pm 0.99 \pm 0.31) \times 10^{-3}$, respectively [76]. Among the CKM favored $b \rightarrow c\bar{u}d$ decays are $\Lambda_b^0 \rightarrow \Sigma_c^0\pi^0$ and $\Xi_b^- \rightarrow \Sigma_c^-K^0$ as well as the $b \rightarrow c\bar{c}s$ decays $\Lambda_b^0 \rightarrow \Xi_c^+D^0$, the CKM suppressed $b \rightarrow u\bar{u}d$ decays $\Xi_b^- \rightarrow \Lambda^0\pi^-$ and $\Lambda_b^0 \rightarrow \Lambda^0K^0$ and the doubly Cabibbo suppressed $b \rightarrow u\bar{u}s$ decays $\Xi_b^- \rightarrow \Xi^0\pi^-$ and $\Lambda_b^0 \rightarrow \Xi^0K^0$. The latter bottom baryon decays are predicted to be severely suppressed according to the SCET analysis of [1]. Again, it would be important to find out whether this prediction shows up in the experimental rates.

A last remark concerns the experimental observability of the decays discussed in this paper. The best way to check on the observability of the decays would be to generate MC events according to the described decay chains and to process them through the detector.

Acknowledgments

This work was funded by the German Bundesministerium für Bildung und Forschung (BMBF) under Project 05P2015 - ALICE at High Rate (BMBF-FSP 202): “Jet- and fragmentation processes at ALICE and the parton structure of nuclei and structure of heavy hadrons”, Carl Zeiss Foundation under Project “Kepler Center für Astro- und Teilchenphysik: Hochsensitive Nachweistechnik zur Erforschung des unsichtbaren Universums (Gz: 0653-2.8/581/2)”, by CONICYT (Chile) PIA/Basal FB0821, by the Russian Federation program “Nauka” (Contract No. 0.1764.GZB.2017), by Tomsk State University competitiveness improvement program under grant No. 8.1.07.2018, and by Tomsk Polytechnic University Competitiveness Enhancement Program (Grant No. VIU-FTI-72/2017). M.A.I. acknowledges the support from PRISMA cluster of excellence (Mainz Uni.). M.A.I. and J.G.K. thank the Heisenberg-Landau Grant for the partial support.

-
- [1] A. K. Leibovich, Z. Ligeti, I. W. Stewart and M. B. Wise, Phys. Lett. B **586**, 337 (2004) [hep-ph/0312319].
 - [2] M. A. Ivanov, M. P. Locher and V. E. Lyubovitskij, Few Body Syst. **21**, 131 (1996).
 - [3] M. A. Ivanov, V. E. Lyubovitskij, J. G. Körner and P. Kroll, Phys. Rev. D **56**, 348 (1997) [arXiv:hep-ph/9612463].
 - [4] M. A. Ivanov, J. G. Körner and V. E. Lyubovitskij, Phys. Lett. B **448**, 143 (1999) [arXiv:hep-ph/9811370].
 - [5] M. A. Ivanov, J. G. Körner, V. E. Lyubovitskij and A. G. Rusetsky, Phys. Rev. D **60**, 094002 (1999) [arXiv:hep-ph/9904421].
 - [6] M. A. Ivanov, J. G. Körner, V. E. Lyubovitskij, M. A. Pisarev and A. G. Rusetsky, Phys. Rev. D **61**, 114010 (2000) [arXiv:hep-ph/9911425].
 - [7] M. A. Ivanov, J. G. Körner, V. E. Lyubovitskij and A. G. Rusetsky, Phys. Lett. B **476**, 58 (2000) [arXiv:hep-ph/9910342].
 - [8] T. Gutsche, M. A. Ivanov, J. G. Körner, V. E. Lyubovitskij and P. Santorelli, Phys. Rev. D **88**, 114018 (2013) [arXiv:1309.7879 [hep-ph]].
 - [9] T. Gutsche, M. A. Ivanov, J. G. Körner, V. E. Lyubovitskij and P. Santorelli, Phys. Rev. D **92**, 114008 (2015) [arXiv:1510.02266 [hep-ph]].
 - [10] T. Gutsche, M. A. Ivanov, J. G. Körner, V. E. Lyubovitskij and P. Santorelli, Phys. Rev. D **93**, 034008 (2016) [arXiv:1512.02168 [hep-ph]].
 - [11] T. Gutsche, M. A. Ivanov, J. G. Körner, V. E. Lyubovitskij, V. V. Lyubushkin and P. Santorelli, Phys. Rev. D **96**, 013003 (2017) [arXiv:1705.07299 [hep-ph]].

- [12] T. Gutsche, M. A. Ivanov, J. G. Körner and V. E. Lyubovitskij, Phys. Rev. D **96**, 054013 (2017) [arXiv:1708.00703 [hep-ph]].
- [13] A. Faessler, T. Gutsche, M. A. Ivanov, J. G. Körner and V. E. Lyubovitskij, Phys. Lett. B **518**, 55 (2001) [hep-ph/0107205].
- [14] A. Salam, Nuovo Cim. **25**, 224 (1962); S. Weinberg, Phys. Rev. **130**, 776 (1963); K. Hayashi, M. Hirayama, T. Muta, N. Seto and T. Shirafulji, Fortsch. Phys. **15**, 625 (1967); G. V. Efimov and M. A. Ivanov, *The Quark Confinement Model of Hadrons*, (IOP Publishing, Bristol & Philadelphia, 1993).
- [15] P. Bialas, J. G. Körner, M. Krämer and K. Zalewski, Z. Phys. C **57**, 115 (1993).
- [16] J. Hrivnac, R. Lednický and M. Smizanska, J. Phys. G **21**, 629 (1995) [hep-ph/9405231].
- [17] A. Faessler, T. Gutsche, M. A. Ivanov, J. G. Körner, V. E. Lyubovitskij, D. Nicmorus and K. Pumsa-ard, Phys. Rev. D **73**, 094013 (2006) [hep-ph/0602193].
- [18] A. Faessler, T. Gutsche, B. R. Holstein, M. A. Ivanov, J. G. Körner and V. E. Lyubovitskij, Phys. Rev. D **78**, 094005 (2008) [arXiv:0809.4159 [hep-ph]].
- [19] A. Faessler, T. Gutsche, M. A. Ivanov, J. G. Körner and V. E. Lyubovitskij, Phys. Rev. D **80**, 034025 (2009) [arXiv:0907.0563 [hep-ph]].
- [20] T. Branz, A. Faessler, T. Gutsche, M. A. Ivanov, J. G. Körner, V. E. Lyubovitskij and B. Oexl, Phys. Rev. D **81**, 114036 (2010) [arXiv:1005.1850 [hep-ph]].
- [21] T. Branz, A. Faessler, T. Gutsche, M. A. Ivanov, J. G. Körner and V. E. Lyubovitskij, Phys. Rev. D **81**, 034010 (2010) [arXiv:0912.3710 [hep-ph]].
- [22] S. Dubnicka, A. Z. Dubnickova, M. A. Ivanov, J. G. Körner, P. Santorelli and G. G. Saidullaeva, Phys. Rev. D **84**, 014006 (2011) [arXiv:1104.3974 [hep-ph]].
- [23] S. Dubnicka, A. Z. Dubnickova, M. A. Ivanov and A. Liptaj, Phys. Rev. D **87**, 074021 (2013) [arXiv:1301.0738 [hep-ph]].
- [24] T. Gutsche, M. A. Ivanov, J. G. Körner, V. E. Lyubovitskij and P. Santorelli, Phys. Rev. D **86**, 074013 (2012) [arXiv:1207.7052 [hep-ph]].
- [25] T. Gutsche, M. A. Ivanov, J. G. Körner, V. E. Lyubovitskij and P. Santorelli, Phys. Rev. D **87**, 074031 (2013) [arXiv:1301.3737 [hep-ph]].
- [26] Y. K. Hsiao, P. Y. Lin, C. C. Lih and C. Q. Geng, Phys. Rev. D **92**, 114013 (2015) [arXiv:1509.05603 [hep-ph]].
- [27] Y. K. Hsiao, Y. Yao and C. Q. Geng, Phys. Rev. D **95**, 093001 (2017) [arXiv:1702.05263 [hep-ph]].
- [28] Fayyazuddin and M. J. Aslam, Phys. Rev. D **95**, 113002 (2017) [arXiv:1705.05106 [hep-ph]].
- [29] J. G. Körner, Nucl. Phys. B **25**, 282 (1971).
- [30] J. C. Pati and C. H. Woo, Phys. Rev. D **3**, 2920 (1971).
- [31] G. Buchalla, A. J. Buras and M. E. Lautenbacher, Rev. Mod. Phys. **68**, 1125 (1996) [hep-ph/9512380].
- [32] W. Altmannshofer, P. Ball, A. Bharucha, A. J. Buras, D. M. Straub and M. Wick, JHEP **0901**, 019 (2009) [arXiv:0811.1214 [hep-ph]].
- [33] M. Neubert, V. Rieckert, B. Stech and Q. P. Xu, In *Heavy Flavours*, Edited by A. J. Buras and M. Lindner (World Scientific, Singapore, 1992), p. 286; HD-THEP-91-28.
- [34] M. A. Ivanov, J. G. Körner, V. E. Lyubovitskij and A. G. Rusetsky, Phys. Rev. D **57**, 5632 (1998) [hep-ph/9709372]; Mod. Phys. Lett. A **13**, 181 (1998) [hep-ph/9709325].
- [35] F. Ambrosino *et al.* [KLOE Collaboration], Phys. Lett. B **648**, 267 (2007) [hep-ex/0612029].
- [36] M. Tanabashi *et al.* (Particle Data Group), Phys. Rev. D **98**, 030001 (2018).
- [37] D. Becirevic, P. Boucaud, J. P. Leroy, V. Lubicz, G. Martinelli, F. Mescia, and F. Rapuano, Phys. Rev. D **60**, 074501 (1999) [hep-lat/9811003].
- [38] D. Bečirević, G. Duplancić, B. Klajn, B. Melić, and F. Sanfilippo, Nucl. Phys. B **883**, 306 (2014) [arXiv:1312.2858 [hep-ph]].
- [39] V. V. Braguta, A. K. Likhoded and A. V. Luchinsky, Phys. Lett. B **646**, 80 (2007) [hep-ph/0611021].
- [40] M. Galanti, A. Giammanco, Y. Grossman, Y. Kats, E. Stamou and J. Zupan, JHEP **1511**, 067 (2015) [arXiv:1505.02771 [hep-ph]].
- [41] T. Mannel and W. Roberts, Z. Phys. C **59**, 179 (1993).
- [42] H. Y. Cheng, Phys. Rev. D **56**, 2799 (1997) [hep-ph/9612223].
- [43] Fayyazuddin and Riazuddin, Phys. Rev. D **58**, 014016 (1998) [hep-ph/9802326].
- [44] R. Mohanta, A. K. Giri, M. P. Khanna, M. Ishida, S. Ishida and M. Oda, Prog. Theor. Phys. **101**, 959 (1999) [hep-ph/9904324].
- [45] A. K. Giri, L. Maharana and R. Mohanta, Mod. Phys. Lett. A **13**, 23 (1998).
- [46] H. Y. Cheng and B. Tseng, Phys. Rev. D **53**, 1457 (1996); Phys. Rev. D **55**, 1697(E) (1997) [hep-ph/9502391].
- [47] C. H. Chou, H. H. Shih, S. C. Lee and H. N. Li, Phys. Rev. D **65**, 074030 (2002) [hep-ph/0112145].
- [48] Z. T. Wei, H. W. Ke and X. Q. Li, Phys. Rev. D **80**, 094016 (2009) [arXiv:0909.0100 [hep-ph]].
- [49] L. Mott and W. Roberts, Int. J. Mod. Phys. A **27**, 1250016 (2012) [arXiv:1108.6129 [nucl-th]].
- [50] R. Aaij *et al.* (LHCb Collaboration), Phys. Lett. B **724**, 27 (2013) [arXiv:1302.5578 [hep-ex]].
- [51] G. Aad *et al.* (ATLAS Collaboration), Phys. Rev. D **89**, 092009 (2014) [arXiv:1404.1071 [hep-ex]].
- [52] CMS Collaboration (CMS Collaboration), CMS-PAS-BPH-15-002.
- [53] H. Y. Cheng and B. Tseng, Phys. Rev. D **46**, 1042 (1992); Phys. Rev. D **55**, 1697(E) (1997).
- [54] J. G. Körner and M. Krämer, Z. Phys. C **55**, 659 (1992).
- [55] P. Zenczykowski, Phys. Rev. D **50**, 402 (1994) [hep-ph/9309265].
- [56] A. Datta, hep-ph/9504428.
- [57] T. Aaltonen *et al.* (CDF Collaboration), Phys. Rev. Lett. **99**, 052002 (2007) [arXiv:0707.0589 [hep-ex]].
- [58] T. Aaltonen *et al.* (CDF Collaboration), Phys. Rev. D **80**, 072003 (2009) [arXiv:0905.3123 [hep-ex]].

- [59] V. M. Abazov *et al.* (D0 Collaboration), Phys. Rev. Lett. **99**, 052001 (2007) [arXiv:0706.1690 [hep-ex]].
- [60] R. Aaij *et al.* (LHCb Collaboration), Phys. Lett. B **736**, 154 (2014) [arXiv:1405.1543 [hep-ex]].
- [61] T. A. Kaeding, “Tables of SU(3) isoscalar factors,” nucl-th/9502037.
- [62] O. Leitner, Z. J. Ajaltouni and E. Conte, Nucl. Phys. A **755**, 435 (2005) [hep-ph/0412131].
- [63] Z. J. Ajaltouni, E. Conte and O. Leitner, Phys. Lett. B **614**, 165 (2005) [hep-ph/0412116].
- [64] R. Aaij *et al.* (LHCb Collaboration), Phys. Rev. Lett. **112**, 202001 (2014) [arXiv:1403.3606 [hep-ex]].
- [65] V. M. Abazov *et al.* (D0 Collaboration), Phys. Rev. Lett. **101**, 232002 (2008) [arXiv:0808.4142 [hep-ex]].
- [66] J. G. Körner and T. Gudehus, Nuovo Cimento **11A**, 597 (1972).
- [67] F. Hussain, J. G. Körner, M. Krämer and G. Thompson, Z. Phys. C **51**, 321 (1991).
- [68] D. A. Varshalovich, A. N. Moskalev and V. K. Khersonsky, *Quantum Theory Of Angular Momentum: Irreducible Tensors, Spherical Harmonics, Vector Coupling Coefficients, 3nj Symbols*, (World Scientific, Singapore, 1988), 514p.
- [69] S. Barlag *et al.* (ACCMOR Collaboration), Z. Phys. C **48**, 29 (1990).
- [70] P. L. Frabetti *et al.* (E687 Collaboration), Phys. Lett. B **314**, 477 (1993).
- [71] J. P. Alexander *et al.* (CLEO Collaboration), Phys. Rev. D **53**, R1013 (1996) [hep-ex/9508005].
- [72] K. Abe *et al.* (Belle Collaboration), Phys. Lett. B **524**, 33 (2002) [hep-ex/0111032].
- [73] A. Zupanc *et al.* (Belle Collaboration), Phys. Rev. Lett. **113**, 042002 (2014) [arXiv:1312.7826 [hep-ex]].
- [74] M. Ablikim *et al.* (BESIII Collaboration), Phys. Rev. Lett. **116**, 052001 (2016) [arXiv:1511.08380 [hep-ex]].
- [75] R. Aaij *et al.* (LHCb Collaboration), Phys. Lett. B **759**, 282 (2016) [arXiv:1603.02870 [hep-ex]].
- [76] M. Ablikim *et al.* (BESIII Collaboration), Phys. Lett. B **783**, 200 (2018) [arXiv:1803.04299 [hep-ex]].